The Flow Structure under Mixed Convection in a Uniformly Heated Vertical Pipe

by

Jeongik Lee

Submitted to the Department of Nuclear Science and Engineering in

partial fulfillment of the requirements for the Degree of

Master of Science in Nuclear Science and Engineering

At the

Massachusetts Institute of Technology

[June 2005]

May 2005

© 2005 Jeongik Lee All rights reserved

MASSACHUSETTS INSTITUTE OF TECHNOLOGY
MAR 2 8 2006
LIBRARIES

ARCHIVES

Author _____

Department of Nuclear Science and Engineering

Certified by _____

Mujid Kazimi, Professor of Nuclear Engineering

Thesis Supervisor

Certified by _____

Pavel Hejzlar, Principal Research Scientist

Thesis Reader

Certified by _____

Pradip Saha, Research Scientist

Thesis Reader

Accepted by _____

Jeff Coderre, Professor of Nuclear Science and Engineering

Chairman, Committee for Graduate Studies

The author hereby grants to MIT permission to reproduce and to distribute publicly paper and electronic copies of this thesis document in whole or in part in any medium now known or hereafter created.

The Flow Structure under Mixed Convection in a Uniformly Heated Vertical Pipe

by

Jeongik Lee

Submitted to the Department of Nuclear Science and Engineering in

partial fulfillment of the requirements for the Degree of

Master of Science in Nuclear Science and Engineering

At the

MASSACHUSETTS INSTITUTE OF TECHNOLOGY

Abstract

For decay heat removal systems in the conceptual Gas-cooled Fast Reactor (GFR) currently under development, passive emergency cooling using natural circulation of a gas at an elevated pressure is being considered. Since GFR cores have high power density and low thermal inertia, relative to the high temperature gas-cooled thermal reactor (HTGR), the decay heat removal (DHR) in depressurization accidents is a major challenge to be overcome. This is due to (1) a gas has inherently inferior heat transport capabilities compared to a liquid and (2) the high surface heat flux of the GFR strongly affects the gas flow under natural circulation. The high heat flux places the flow into a mixed convection regime, which is not yet fully understood. One of the issues of mixed convection is that the transition from laminar to turbulent flow is not clearly defined in the existing literature. Review of previous work on heat transfer mechanisms and flow characteristics of the mixed convection transitional regime shows that two transitional zones exist between laminar or laminar-like flow and fully turbulent flow for the upward heated case. Previous work has focused on liquids and thus is not applicable to gas mixed convection. An experimental facility is designed to obtain the data in the regions not covered in previous work, using nitrogen, helium and carbon dioxide. The facility is expected to operate with heat fluxes up to $10kW/m^2$ and gas velocities up to 2.5m/s by natural circulation only. A velocity calibration method is designed in addition to the hot-wire probe for velocity and temperature profiles measurement. Finally, computational simulations, using the commercial code FLUENT, are performed to select an appropriate turbulence model for investigating mixed convection transitional flow regimes. It was concluded that the basic models in FLUENT were not capable of predicting the transitional flow as the Launder-Sharma turbulence model does. Nevertheless, the advanced numerical algorithm and convenient postprocessor of FLUENT can still be utilized by using UDF to incorporate other turbulence models into the code.

Thesis Advisor: Prof. Mujid S. Kazimi

Title: Professor of Nuclear Engineering

ACKNOWLEDGEMENTS

This work was partially supported by Idaho National Laboratory under the Strategic INL/MIT Nuclear Research Collaboration Program for Sustainable Nuclear Energy. The author would also like to acknowledge the financial support he received from a fellowship provided by the Korean Ministry of Science. The author would also like to thank Prof. Mujid S. Kazimi, Dr. Pavel Hejzlar, Dr. Pradip Saha and Mr. Pete Stahle for their suggestions and guidance. In addition, several comments by Dr. Don McEligot of INL are also appreciated.

TABLE OF CONTENTS

LIST OF FIGURES

LIST OF TABLES

NOMENCLATURE

c_p: specific heat

g: gravitational acceleration

g_c : force-mass conversion factor

h: heat transfer coefficient

k: thermal conductivity

k_J, h_J : Jorgensen's Law Coefficients

n : King's Law Coefficients

q''_w: wall heat flux

r : radial direction

x: axial distance

y: distance from the wall

A, B : King's Law Coefficients

A_s : stability parameter [Hanks, 1963] $= \dfrac{2\rho\left|U\, dU/dr\right|}{g_c\left|\nabla\cdot\tau\right|}$

D: pipe diameter

E : Response of hot-wire

G: mass flux

T: temperature

U: axial velocity component

V : Velocity

α: thermal diffusivity $= \dfrac{k}{\rho c_p}$

β: thermal expansion coefficient $= -\dfrac{1}{\rho}\left(\dfrac{\partial\rho}{\partial T}\right)_P$

τ: wall shear stress $= \rho\nu\left.\dfrac{\partial U}{\partial y}\right|_{y=0}$

ν : kinematic viscosity

ρ: density

Bo: buoyancy parameter [Jackson et al., 1989] $= 8\times10^4\,\dfrac{\mathrm{Gr_q}}{\mathrm{Re_f^{3.425}\,Pr_f^{0.8}}}$

$Gr_{\Delta T}$: Grashof number = $\frac{g\beta(T_w - T_b)D^3}{\nu^2}$

Gr_q : Grashof number with heat flux = $Gr_{\Delta T}Nu = \frac{g\beta q''_w D^4}{k\nu^2}$

K: acceleration parameter = $\frac{\nu}{U_b^2}\frac{dU_b}{dx} \approx \frac{Gr_{\Delta T}}{2Re^3} \approx \frac{4q_b^+}{Re}$

Nu: Nusselt number = $\frac{hD}{k}$

Pr: Prandtl number = $\frac{\nu}{\alpha}$

Ra: Rayleigh number = $Gr_{\Delta T}$ Pr

Ra^* : Modified Rayleigh number [Churchill, 1998] = $\frac{\rho g \beta c_p D^4}{\nu\alpha}\left(\frac{dT_b}{dx}\right)$

Re: Reynolds number = $\frac{UD}{\nu}$

q^+: nondimensional heat flux = $\frac{q''_w}{Gc_pT}$

u^+: nondimensional velocity = $U\sqrt{\frac{\rho}{\tau}}$

y^+: nondimensional wall coordinate = $\frac{y}{\nu}\sqrt{\frac{\tau}{\rho}}$

Subscript

b: bulk
f: film
m: mixed convection
w: wall
bi : binormal component
cr: critical point of transition
df: downflow
in: inlet
no: normal component
up: upflow

ta: tangential component

eff : effective cooling velocity

F : forced convection

N : natural convection

1 INTRODUCTION

1.1 DESCRIPTION OF GENERAL THERMAL HYDRAULIC FEATURES OF A GFR

The gas-cooled fast reactor (GFR) is a candidate for the next generation reactors. The GFR is often compared with the high temperature gas-cooled thermal reactor (HTGR), since both utilize gaseous coolants at high core outlet temperatures. However, GFR and HTGR have many differences not only in neutronics, but also in thermal-hydraulic behavior.

Since Generation IV sets high targets for safety, a passive cooling system that does not rely on an emergency power supply is seriously considered for GFR decay heat removal (DHR). One of the thermal-hydraulic characteristics of GFR is that it is designed for about ten times higher power density than HTGR to achieve good economy. Another characteristic of the GFR is its low thermal inertia due to the absence of moderator, such as graphite. These characteristics require reliance on more efficient heat transfer mechanisms for the DHR than only conduction and radiation as used in HTGR. One such mechanism under investigation is natural circulation of a gas coolant through a loop connecting the core with an elevated heat exchanger [Williams et al., 2004].

A gas system that removes heat by natural circulation is challenging to design due to inherently low heat transport capabilities of the gas. Moreover, passive systems with high heat fluxes can easily experience various regimes, such as a mixed convection regime, in a transient situation whereas most of the industrial energy systems typically are designed to operate in forced convection regime [Williams et al., 2004]. In order to design and build such DHR systems, it is essential to have reliable heat transfer and friction factor correlations or adequate computational fluid dynamics (CFD) tools for all possible flow

regimes. It is clear that these correlations could only be obtained through a thorough understanding of actual physical phenomena backed up by good experimental data.

The objective of this work is to summarize the results of previous investigations and identify the areas with least understanding where further research should be more focused should be more focused on to understand the mechanism of ambiguous flow regimes such as a mixed convection. The study will further provide the basis for construction of experimental facility that can close the gaps in knowledge of heat transfer in these regimes. The experimental facility design and part of the numerical analysis results will be also shown in the thesis, since both the experiment and numerical analysis approaches will be pursued.

1.2 DEFINITION OF FLOW REGIMES

Convection can be divided into three regimes: forced, mixed and natural convection. These terms will be defined briefly to avoid any future misunderstandings, even though these terms are well known to many readers.

Forced convection is the flow that is driven by an externally imposed pressure difference. The heat transfer coefficient and friction factor for such flows strongly depend on the Reynolds number and Prandtl number. By definition, even in a closed loop where there is a heat source and a heat sink but no pump or blower to drive the flow, forced-convection flow can be achieved by having a large buoyancy head due to a density gradient induced by a temperature difference between the heat source and sink. In other words even in "natural circulation flow", heat may be removed from the source by forced convection, if the globally induced flow is large enough so that the local buoyancy force affecting the velocity field is small in the individual channels. In short, categorization of convection regimes depends more on the local effects, rather than the overall or global system behavior.

Natural or free convection, on the other hand, can be defined as the flow that is driven by the local buoyancy force induced by the wall-to-bulk temperature difference, and the characteristic governing nondimensional parameters are the Grashof number and Prandtl number. Since there is no imposed external pressure gradient, the velocity field solution totally depends on the local density gradient caused by the temperature field.

Mixed convection is defined when both the flow and temperature are affecting each other

and none of the terms in the momentum and energy equations can be easily neglected. Therefore, typical governing non-dimensional numbers are the Reynolds number, Grashof number and Prandtl number. Throughout the literature other important non-dimensional numbers, such as the non-dimensional heat flux, buoyancy parameter, acceleration parameter, etc. are frequently used by different investigators. However, most of these can be expressed as combinations of Grashof, Reynolds and Prandtl numbers.

Since the momentum and energy equations are non-linear, simply adding the forced convection and natural convection solution linearly is not a reasonable approach for mixed convection solutions. Also if the fluid properties, for example viscosity, change significantly with temperature and pressure, which is typical for supercritical fluid or gas, the problem becomes even more complex, compared to the forced or natural convection alone. In addition, it can be seen that forced convection and natural convection are the two extremes of the more general case of mixed convection.

Convection regimes can be subdivided into three flow regimes: laminar, transitional and turbulent flow. These flow regimes will be briefly defined as: laminar flow is a stable flow, turbulent flow is an unstable flow and transitional flow is when flow develops from laminar to turbulent flow or vice versa. Physically, viscous shear and molecular conduction are the major mechanisms that transfer momentum and heat in the laminar flow. In the turbulent flow, the unstable nature of the flow enhances the transport of the momentum and heat compared to a stable laminar flow [Kays et al. 1993].

By these definitions, we can categorize the whole flow regime into nine overlapping areas: laminar forced convection, laminar mixed convection, laminar natural convection and so

forth as shown in Table 1-1. A GFR passive decay heat removal system is likely to operate in most of these nine flow regimes during transient conditions [Williams et al. 2004]. To evaluate the performance of the designed system with sufficient accuracy, knowledge of these flow regimes is necessary, since heat transfer mechanisms and characteristics are expected to be different in different regimes.

Among these nine regimes, I will specifically focus on the transitional flow in the mixed convection regime, since only limited data and theoretical analysis are available for this regime compared to the other regimes, as will be explained in detail next.

TABLE 1-1 FLOW REGIMES

	Laminar Flow	Transitional Flow	Turbulent Flow
Forced Convection	X	X	X
Mixed Convection	X	X	X
Natural Convection	X	X	X

2 LITERATURE REVIEW

Good review articles on general mixed convection exist, such as the work of Kakac et al. [1987], Jackson et al. [1989] and Vilemas et al. [1991]. Most of the articles refer to the well-known Metais-Eckert flow regime map [Metais et al., 1964] shown in Figure 2-1. However, the purpose here is to focus more on the transitional flow regime, which was not clearly covered in those review papers.

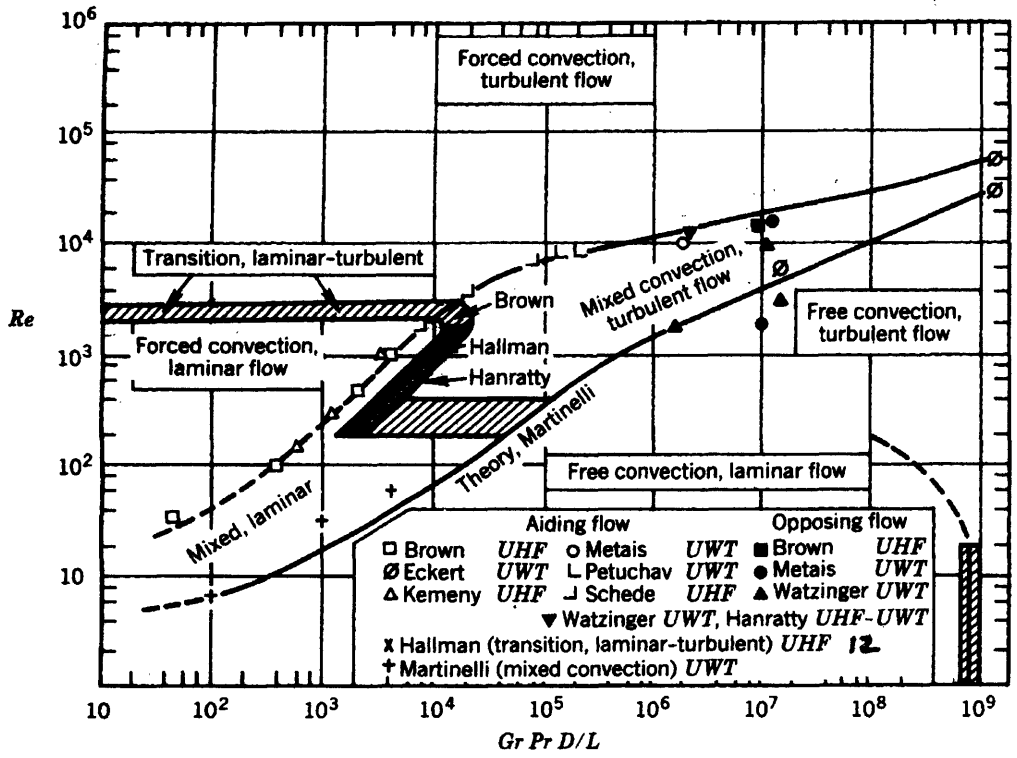

FIGURE 2-1 METAIS & ECKERT FLOW REGIME MAP [METAIS ET AL., 1964]

The present literature search was restricted to upflow in a heated vertical tube or pipe geometry to resemble GFR block core coolant channels, i.e., the flow direction is the same as that induced by the buoyancy force, which is also called "aiding flow" in the literature.

Mixed convection "aiding" flow received much attention in the past decades because, for

certain conditions, the heat transfer coefficient can drop significantly and the wall temperature can exhibit considerable increases [Jackson et al. 1989]. An explanation of this fluid behavior was provided by Jackson et al. [1989] as follows. As the heating increases, the heat transfer is deteriorated due to three different mechanisms: (1) the local buoyancy effect that decreases the generation of turbulence within the boundary layer due to a shear stress redistribution (2) acceleration of the main flow due to the bulk density decrease and (3) the variation of the fluid properties such as thermal conductivity, viscosity and so forth. Subsequently, the turbulence production in the boundary layer diminishes, and the turbulent flow behaves more or less like a laminar flow. This is called "laminarization". But after passing through the laminarization point, further increases in the buoyancy force enhance heat transfer compared to that due to forced convection alone. To summarize briefly, turbulence loses its strength at high heat transfer compared to laminar flow due to a decrease in eddy motion in a certain range of the buoyancy effect.

However, the issue is that even though the mechanism itself is clear enough, the analyses in the vast amount of literature are not consistent. Different researchers used different sets of non-dimensional groups to explain the behavior and the correlations were limited to a certain range of parameters only, which suggests that the problem is still not fully resolved in terms of quantitative analysis.

The main issue, which is going to be introduced in the following text, is that at least two transitional zones exist in the mixed convection regime. The first one is the transition from laminar to turbulent flow, and the second one is the transition from turbulent to laminarized flow, which is the mechanism discussed above. However, differentiation between the two transitional zones is not clearly stated in the literature, and there is not much experimental

evidence to prove that two transitional zones exist. Thus, the author focuses on the transitional flow in mixed convection regime where we have the least understanding.

Since gas viscosity increases as the temperature increases, which is exactly opposite to that of a liquid, the gas and liquid behavior may have some differences in the transition range [Herwig et al., 1992]. Thus, references that deal with liquids and gases are separated. However, it should be noted that because this work emphasizes GFR conditions, the references that concentrate on mixed convection in gas flow regime will get more attention than the liquid side. References will be reviewed in the order of mixed convection in laminar, turbulent, transition from laminar to turbulent and transition from turbulent to laminarized turbulent or laminar-like flow.

2.1 LAMINAR FLOW IN MIXED CONVECTION

Liquid

Hallman [1955] analytically solved for the velocity and temperature profiles for fully developed laminar flow with internal heat generation. Since the main assumption was that the flow was fully developed, the inertia terms were neglected and the flow had only axial velocity, which is the same as a one-dimensional flow.

These results were expanded and verified in Hallman's later work [Hallman, 1961]. Experimental data was compared to analysis and showed reasonable agreement. However, the experiment was performed with water. Hallman [1961] also included developing length correlation, transition condition from laminar to turbulent flow and a Nusselt number correlation. The developing length and transition condition are used in the later part of this work, in order to transform other transition conditions and compare them to each other.

Churchill [1998] suggested heat transfer correlations for different flow regimes and orientations, including laminar mixed convection for aiding flow. The suggested correlation for the laminar mixed convection region was tested with the Hallman's data [1961] and it fitted the data with lesser error than what Hallman originally suggested in his work. Equation (2-1) is the correlation, which Churchill suggested in his work.

$$\mathrm{Nu}^6 = \mathrm{Nu}_F^6 + \mathrm{Nu}_N^6 \tag{2-1}$$

$$\mathrm{Nu}_F = \frac{48}{11},\ \mathrm{Nu}_N = 0.846\left(\mathrm{Ra}^*\right)^{1/4} \text{ where } \mathrm{Ra}^* = \frac{\rho g \beta c_p D^4}{\nu \alpha}\left(\frac{dT_b}{dx}\right)$$

From the correlation it is clearly seen that Churchill superimposed forced convection and natural convection heat transfer coefficient nonlinearly to get the mixed convection heat transfer coefficient, which seems successful for laminar aiding flow mixed convection case. However, though Churchill tried the same technique for developing a turbulent aiding flow mixed convection heat transfer correlation, it has a cusp point in the correlation which is not favorable to implement in the system analysis codes such as RELAP5.

Gas

Worsøe-schmidt and Leppert [1965] and Worsøe-schmidt [1966] approached the problem numerically by employing an implicit finite difference method. The momentum equation included the inertia term and it was solved for two-dimensional velocity field, which was different from Hallman's work [1955]. The difference between the two studies, namely [Worsøe-schmidt & Leppert, 1965] and [Worsøe-schmidt, 1966], is in the different working fluids: the first one used air, and the other used helium and carbon dioxide, but the approach was the same. The data that are presented in these papers are going to be compared with the experiments to be performed at MIT, as explained in detail later.

Zeldin and Schmidt [1972] performed numerical analysis and experiments with air for Reynolds number in the range of 300 to 500 in 40mm inner diameter tube. The momentum equation for the numerical analysis included more terms than Worsøe-schmidt and Leppert [1965] did. The boundary condition was uniform wall temperature, which is different from all the other papers that are introduced in this thesis. In addition the velocity and temperature profiles were measured by using a hot-film probe.

Nesreddine et al. [1998] performed numerical analysis like Worsøe-schmidt and Leppert [1965] did, but the main governing equations were the same as the work of Zeldin and Schmidt [1972] except for the boundary condition; the uniform wall heat flux boundary condition was used. The main interest of the paper was to define the effects of axial diffusion on laminar heat transfer, and this led them to set criteria to determine when the upstream boundary conditions can be applied at the entrance of the heated section and when the elliptical formulation is necessary to describe the flow field accurately. Worsøe-schmidt and Leppert's work [1965] can be checked against this result to find out if there is a problem for the Worsøe-schmidt and Leppert result [1965] due to neglecting some terms in the momentum equation.

As a conclusion, for laminar mixed convection aiding flow, it seems that most of the work concentrated more on the numerical analysis than the experiment. The only existing data are for the liquid side and the heat transfer correlation that can be readily used is the one that Churchill [2003] suggested (Equation 2-1). Therefore it is suggested that before applying Churchill's correlation for the design of a gas-cooled system, gas flow experiments need to be conducted to verify the applicability.

2.2 TURBULENT FLOW IN MIXED CONVECTION

For defining turbulent mixed convection, some inconsistencies among various literature sources arise regarding the governing non-dimensional groups, and these problems should be stated before going into the actual review.

The first issue is inconsistency of the definition of the buoyancy parameter. The Hall and Jackson [1969] definition followed by other works such as Jackson et al. [1989], Parlatan et al. [1996] and Celata et al. [1998] are different from that of Aicher and Martin [1997]. This will be discussed later.

The second issue involves the fluid properties that should be used for the non-dimensional groups. For instance Poškas et al. [1989] correlation evaluates non-dimensional heat flux based on inlet condition, while other works such as Bankston's non-dimensional heat flux [1970] is defined with local bulk fluid properties.

The last issue is consideration of the axial length to diameter ratio effect. Metais and Eckert [1964] include this effect for plotting their flow regime map; Aicher and Martin [1997] and Celata et al. [1998] tested the effect and showed changes in the heat transfer coefficient with varying ratio of length to diameter. Bankston [1970] and Vilemas et al. [1992] also considered this effect in their papers. But others such as Carr et al. [1973] and Shehata and McEligot [1998] do not use a non-dimensional group that includes this effect, since they were measuring with only one diameter test section. In addition Cotton and Jackson [1990] and Parlatan et al. [1996] did not include this effect without any comparison or reasoning.

It should also be noted that the turbulent mixed convection includes the laminarized turbulent flow. But the papers that are discussed here do not explicitly suggest a transition criterion between the turbulent and laminarized turbulent flow regimes.

Liquid

Parlatan et al. [1996] measured the friction factor and Nusselt number with water experiement. The measured heat transfer coefficient and friction factor reasonably matched other data that were taken from previous gas experiments. This paper also takes into account the effect of property variation with temperature to see buoyancy effect only.

Aicher and Martin [1997] started with a review of previous work and introduced a buoyancy parameter, which was defined as the ratio between the natural convection boundary layer thickness and the forced convection boundary layer thickness (Equation 2-2).

$$\frac{Ra^{0.333}}{Re^{0.8}\,Pr^{0.4}} \tag{2-2}$$

This definition is different from Hall and Jackson's definition [1969], which is further developed in [Jackson et al., 1989] (Equation 2-3).

$$Bo=8\times10^{4}\,\frac{Gr_q}{Re_f^{3.425}\,Pr_f^{0.8}} \tag{2-3}$$

The difference comes from how they derived the non-dimensional parameter. Hall and Jackson developed the buoyancy parameter based on the shear stress modification due to the buoyancy force while Aicher and Martin simply took the ratio of the natural convection and forced convection boundary layer thicknesses.

Aicher and Martin [1997] also suggests a new form of Nusselt number correlation by correlating the opposing flow to the aiding flow using the Gauss equation for fitting their data, which seemed successful. But the way that the correlation was constructed raises some questions. They superimposed the forced convection Nusselt number and the natural convection Nusselt number nonlinearly to obtain an opposing flow Nusselt number and this is used in estimating the aiding flow Nusselt number. However, since the length to diameter ratio effect is included only in forced convection, and considering that the length to diameter ratio also has a strong effect on natural convection, the constructed correlation may not capture the length-to-diameter effect correctly [Celata et al., 1998].

Part of the reason why natural convection Nusselt number correlation for turbulent flow seems incomplete is that the correlation for vertical tube is not readily found in the literature. It is rare to find the justification for using a vertical plate correlation for a vertical tube, by simply changing the geometrical parameter [Churchill, 1998]. Still Yan and Lin [1991] provide limited experimental data and numerical analysis results on this topic. It would be valuable if other researchers perform experiments and corresponding analyses to validate the data and correlation of Yan and Lin [1991], before the heat transfer correlation for the natural convection in tube can be accepted for design purposes.

Celata et al. [1998] followed a similar approach to that of Aicher and Martin [1997]. They

incorporated the length to diameter ratio effect into their correlation by fitting a parameter as a function of the length to diameter ratio, which is constructed from their own experimental data. They showed that the Nusselt number for aiding flow depends on the buoyancy parameter defined by Hall and Jackson [1969] and on the length to diameter ratio. Celeta et al.'s correlation is given below (Equation 2-4). It is a recently developed correlation for the mixed convection turbulent flow of water including the laminarized turbulent flow and captures most of the important physical mechanism of the flow.

$$\frac{\mathrm{Nu}_{\mathrm{m,up}}}{\mathrm{Nu}_{\mathrm{m,df}}} = \psi \tag{2-4}$$

$$\psi = 1 - a\exp\left\{-0.8\left[\log\left(\frac{\mathrm{Bo}}{b}\right)^2\right]\right\},\quad a = 0.36 + 0.0065\frac{L}{D},\quad b = 869\left(\frac{L}{D}\right)^{-2.16}$$

$$\mathrm{Nu}_{\mathrm{m,df}}^3 = \mathrm{Nu}_{\mathrm{F}}^3 + \mathrm{Nu}_{\mathrm{N}}^3;\quad \mathrm{Nu}_{\mathrm{F}} = 0.023\,\mathrm{Re}_b^{0.8}\,\mathrm{Pr}_b^{0.4}\left(\frac{\mu_b}{\mu_w}\right)^{0.11};\quad \mathrm{Nu}_{\mathrm{N}} = \frac{0.15\left(\mathrm{Gr}_{\Delta\mathrm{T}}\,\mathrm{Pr}_w\right)^{1/3}}{\left(1+\left(0.437/\mathrm{Pr}_w\right)^{9/16}\right)^{16/27}}$$

Gas

Steiner [1971] measured the time-average velocity and temperature profiles with a hot-wire for Reynolds numbers between 5,000 and 15,000 in a 80mm inner diameter tube using air as the working fluid. He calculated the acceleration parameter by following the original definition (Equation 2-5) and showed that the buoyancy force induced flow accerleration plays a significant role for the reverse transition from turbulent flow to laminar-like flow by the change in velocity and temperature profiles.

$$K = \frac{\nu}{U_b^2}\frac{dU_b}{dx} \tag{2-5}$$

Carr et al. [1973] also measured the velocity and temperature profiles of air by using a hot-wire in the Reynolds number range from 5,000 to 14,000 in a 88mm inner diameter test section. But they obtained additional data for the fluctuating velocity and temperature profiles at various radial positions, which showed that the viscous sublayer increases at higher heat fluxes. The friction factor and heat transfer rate change because the viscous sublayer thickens.

Polyakov and Shindin [1988] presented their air data for the turbulent transport quantities and heat transfer for 5,000 and 9,000 Reynolds numbers in a 46mm inner diameter test section. Their work showed that the turbulent heat transport is more suppressed than the momentum transfer, which in turn leads to significant reduction of heat transfer rate while there is relatively small change in friction.

Vilemas et al. [1992] showed a construction of the Nusselt number correlation based on a buoyancy parameter, which is defined differently (Equation 2-6) from Hall and Jackson [1969] and Aicher and Martin [1997] and non-dimensional heat flux by fitting their experimental data. They also agreed that the length to diameter ratio affects the heat transfer rate and included it in the correlation. However, they failed to obtain correlation when natural convection plays a significant role. Air experiments were performed in the Reynolds number range from 3,000 to 50,000.

$$\text{Thermo Gravitational Parameter} = \frac{Gr_q}{4Re^3 Pr} \qquad (2\text{-}6)$$

Poškas et al. [1993] measured the time-average and fluctuating velocity and temperature profiles for the Reynolds number 11,400 in air. They reached similar conclusion of Carr et

al. [1973] and Polyakov and Shindin [1988], confirming that suppressed generation of the turbulence near the wall causes the heat transfer rate deterioration.

Shehata [1984] and Shehata and McEligot [1998 and 1995] measured the time-average velocity and temperature profiles but at lower Reynolds numbers of 4,000 and 6,000 using air at higher heating rates than in the previously mentioned papers. Thus the velocity and temperature profiles were more distorted by the increased influence of buoyancy or natural convection effects.

In addition to the experimental work above, the turbulent mixed convection has been also studied numerically. Cotton and Jackson [1990] performed numerical analysis with Launder and Sharma k-ε model, which is designed for low Reynolds number. They compared their result with the data of Steiner [1971], Carr et al. [1973] and others, in order to verify the model. The model seems to perform reasonably well for predicting the experimental data.

You et al. [2003] utilized direct numerical simulation (DNS), which is a relatively new method for engineering analysis, and compared it to other turbulence models. Their calculation results were compared to the data of Carr et al. [1973], Polyakov and Shindin [1988] and Parlatan et al. [1996] for aiding flow experiment along with other papers that include opposing flow experimental data. DNS results showed reasonable agreement with the data, but since DNS requires tremendous amount of computational power, the case study is limited in comparison with other turbulence models.

Satake et al. [2000], Mikielewicz et al. [2002], Xu et al. [2004] and Spall et al. [2004]

compared their calculations to the experimental data of Shehata et al. [1998]. Satake et al. [2000] used DNS, which is similar to the work of You et al. [2003]. Mikielewicz et al. [2002] compared various turbulence models that fall into a modified version of k-ε model and k-τ model for low Reynolds number. Xu et al. [2004] obtained their results using the large eddy simulation technique (LES), which is another newly developed method like DNS. Finally, Spall et al. [2004] compared k-ω and v^2-f low Reynolds turbulence models. DNS and LES showed reasonable agreement with the experimental data of Shehata and McEligot [1998]. Mikielewicz et al. [2002] concluded that the Launder-Sharma (L-S) turbulence model is the best fitting model and Spall et al. [2004] concluded that the v^2-f low Reynolds turbulence model performs better than the k-ω and Launder-Sharma models.

As a summary of this section, two points are made.

1. A larger number of Nusselt number correlations have been developed for liquids in contrast to the gas. On the other hand, vast amount of data have been obtained for gases for the studies of turbulence structure. So far Equation 2-4 developed for water is the best heat transfer coefficient correlation that encompasses all the physical attributes of the mixed convection phenomena. However, Equation 2-4 needs to be validated with gas experiments before it can be applied to the GFR design.

2. Carr et al. [1973], Petukhov and Polyakhov [1988] and Parlatan et al. [1996] showed some data and correlation for mixed convection turbulent flow friction factor. However since the data and correlation are somewhat inconsistent, verification is required before implementing the correlation into a system analysis

code. It is likely that the friction factor is related to the heat transfer coefficient, and this means that accurate friction factor correlation may lead us to a better Nusselt number correlation for both liquid and gas flows.

2.3 TRANSITIONAL FLOW IN MIXED CONVECTION

2.3.1 Transition from Laminar to Turbulent Flow

One of the earliest attempts to predict the instability of the non-isothermal pipe flow was by Scheele and Greene [1966]. They predicted the instability by applying a local dimensionless stability parameter (Equation 2-7), developed by Hanks [1963], with the Hallman [1955] velocity profile.

$$A_s = \frac{2\rho|u\, du/dr|}{g_c|\nabla \cdot \tau|} \tag{2-7}$$

One of the tabulated experimental data shows that with liquid even for very low Reynolds numbers, between 5 and 20, a flow instability may develop due to the high heating rate. This early laminar-to-turbulent transition is not the same as the laminarization phenomenon, i.e. transition from turbulent to laminarized turbulent or laminar-like flow. This will be explained more clearly when we review the work of Chen and Chung [2003].

Herwig and Schäfer [1992] applied the classical linear stability theory to include temperature and pressure dependence of the fluid properties in heated upflow along a flat plate. The results show that decreasing the viscosity in the near-wall region of the boundary layer stabilizes the flow, whereas the flow would be destabilized when the viscosity decreases uniformly across the whole flow. This gives a clue that the liquid transition Reynolds number from laminar to turbulent may be higher for heated flow than for the non-heated flow, since liquid viscosity decreases with temperature, while the gas transition Reynolds number will behave reversely since the viscosity increases with

temperature.

Behzadmehr et al. [2003] used the Launder-Sharma (L-S) turbulence model [Launder et al., 1974] to predict the transition condition from laminar to turbulent flow for gas flow in a heated pipe. They assumed that if the calculated turbulence kinetic energy diminishes to zero, the whole flow can be laminar and when the turbulence kinetic energy starts to grow then the flow falls into the transitional flow region and becomes turbulent flow. From their numerical prediction it seems that the transition from laminar to turbulent flow occurs even in low Reynolds number due to the heating, which is a similar conclusion with the other works. However, the calculation results will be discussed further when laminarized flow references are reviewed.

Chen and Chung [2003] utilized DNS for investigating how instability grows when the flow is heated. The geometry setup is parallel plate, which is closer to a pipe than what Herwig and Schäfer [1992] assumed. It is found that in buoyancy-aiding situation, the buoyancy force disturbs the flow even at low Reynolds numbers and accelerates the instability growth. However, fluid properties' variation with temperature and pressure should be included to compare to the results of Herwig and Schäfer [1992] and determine whether the liquid and gas behave differently.

From these reviews one can observe with limited evidence that the critical Reynolds number for transition from laminar to turbulent flow in a pipe with gas may be lower for heated aiding flow but this conclusion is restricted to numerical results. Even though the experimental data that were presented by Scheele and Greene [1966] gave some clues to the problem, the data were limited to liquids. Gases may behave differently.

2.3.2 Transition from Turbulent to Laminarized Turbulent Flow

The criterion for transitional conditions for "laminarization" is somewhat ambiguous. For example, Tanaka et al. [1987] and Kaupas et al. [1989] present their criterion that includes the laminar-to-turbulent and "laminarization" transitional zones together. In the previous section, it was shown that the physical basis of the shift in critical Reynolds number for the first transitional zone is different from the second transitional zone. The first shift in critical Reynolds number occurs from the disturbance or turbulence that is created by heating, and the second shift comes from reduced turbulence due to further heating of the flow. But this difference is not clearly stated in the literature.

Bankston [1970] performed an experiment in a tube with the entrance Reynolds numbers from 2,350 to 12,500 and obtained the friction factor and local heat transfer coefficient data for hydrogen and helium. This paper is focused on the laminarization criterion where turbulent flow changes to laminar-like flow. The condition is given in terms of the acceleration parameter, which can be calculated approximately by the ratio between non-dimensional heat flux and Reynolds number [McEligot et al., 1969].

$$K = \frac{\nu}{U_b^2}\frac{dU_b}{dx} \approx \frac{4q_b^+}{\mathrm{Re}} \qquad (2\text{-}8)$$

[McEligot et al., 1969]

Tanaka et al. [1987] implemented low Reynolds k-ε model, which is a modified version of Jones and Launder model by Kawamura, and generated a flow regime map via their numerical calculations. They interpreted the acceleration parameter in a unique way and

this interpretation is going to be used in this thesis. They also performed a simple experiment with nitrogen to prove their calculation results, and the experiment range covered Reynolds numbers between 2,900 and 5,000.

$$K = \frac{\nu}{U_b^2}\frac{dU_b}{dx} \approx \frac{\mathrm{Gr}_{\Delta T}}{2\mathrm{Re}^3} \tag{2-9}$$

[Tanaka et al., 1987]

Kaupas et al. [1989] focused on the development of the transitional Reynolds number, which changes with increasing heat flux, and the heat transfer correlation in the transitional flow. The correlation seems to fit well with the experimental data, but the correlation itself is based on inlet fluid properties rather than local properties. They claim that their correlations for transitional Reynolds number are from the laminar to turbulent flow rather than turbulent to laminarized flow.

There are two main issues in the comparison of different types of correlations. The first issue is omission of the dependency of axial position, even though length-to-diameter ratio is important in mixed convection regime [Celata et al., 1998], and it is solved by assuming fully developed flow in order to express x/d in terms of the Reynolds number and Prandtl number [Hallman, 1961]. For high Rayleigh number flow, Hallman [1961] proposed the following expression for the fully-developed flow condition.

$$\frac{2x}{D\,\mathrm{Re}\,\mathrm{Pr}} = 0.034 \tag{2-10}$$

[Hallman, 1961]

This is just a temporary solution to the issue, since the Hallman [1961] correlation was based on water experiments, which may have different behavior than gas. Also the fully developed length was for the laminar flow only, not for other flow regimes, which can be another source of error. However, the whole purpose of this attempt is to put various "laminarization" transition conditions into one map to capture buoyancy effects, in order to compare their general trend to each other, not to obtain exact mapping.

The second problem is the conversion of heat flux based acceleration parameter to the temperature based acceleration parameter. By equating Tanaka et al.'s [1987] interpretation of acceleration parameter to McEligot et al.'s [1969] interpretation of the parameter, the conversion problem is solved. Tanaka et al. [1987] used the film temperature for the Grashof number, and this is the reason why it is divided by two in order to evaluate the Grashof number based on the bulk temperature.

$$K = \frac{\nu}{U_b^2}\frac{dU_b}{dx} \approx \frac{\mathrm{Gr}_{\Delta T}}{2\mathrm{Re}^3} \approx \frac{4q_b^+}{\mathrm{Re}} \tag{2-11}$$

[Tanaka et al., 1987] and [McEligot et al., 1969]

The two methods were applied to each transition condition. Next part shows the procedure, which was applied to convert each condition to a comparable form.

Tanaka et al. Laminarization Transition Criterion

$$\frac{\mathrm{Gr}_{\Delta T}}{2\mathrm{Re}^3} = 3\times10^{-6} \quad \Leftrightarrow \quad \mathrm{Re} = \left(\frac{\mathrm{Ra}}{6\times10^{-6}\,\mathrm{Pr}}\right)^{\frac{1}{3}} \tag{2-12}$$

Bankston Laminarization Transition Criterion

$$K = \frac{4q_b^+}{\mathrm{Re}} = 2\times10^{-4}(0.021\mathrm{Re}^{-0.2}\,\mathrm{Pr}^{-0.6}) \Leftrightarrow \quad \mathrm{Re} = \left(\frac{\mathrm{Ra}}{8.4\times10^{-6}\mathrm{Pr}^{0.4}}\right)^{\frac{1}{2.8}} \tag{2-13}$$

Kaupas et al. Transition Criteria

$$\mathrm{Re} = 3.07\,\mathrm{Re}_{cr}(q_{in}^+)^{0.125}$$

$$\text{where } \mathrm{Re}_{cr} = 3250 \text{ Laminarized to Transtional Flow}$$
$$= 4100 \text{ Transtional to Turbulent Flow} \tag{2-14}$$

since,

$$q_b^+ = \frac{q_w''}{Gc_pT_b} = \frac{q_w''}{Gc_pT_{in} + q_w''\dfrac{\pi Dx}{\dfrac{\pi}{4}D^2}}$$

$$\Leftrightarrow \quad \frac{q_{in}^+}{q_b^+} = 1 + q_{in}^+\frac{4x}{D} \Leftrightarrow \quad q_b^+ = \frac{q_{in}^+}{1+q_{in}^+\dfrac{4x}{D}} = \frac{\mathrm{Ra}}{8\mathrm{Re}^2\,\mathrm{Pr}} \tag{2-15}$$

By applying the fully developed condition to approximate non-dimensional heat flux evaluated from the inlet condition to non-dimensional groups based on fully developed condition, we get

$$q_{in}^{+} = \frac{1}{8}\left(\frac{1}{\frac{\mathrm{Re}^2\,\mathrm{Pr}}{\mathrm{Ra}} - 0.017\,\mathrm{Re}\,\mathrm{Pr}} \right) \tag{2-16}$$

Inserting this equation into the correlation of Kaupas et al., we obtain

$$\mathrm{Re}^{10} - 0.017\mathrm{Ra}\,\mathrm{Re}^{9} - \frac{\left(3.07\,\mathrm{Re}_{cr}\right)^{8}}{8}\frac{\mathrm{Ra}}{\mathrm{Pr}} = 0 \tag{2-17}$$

This equation has one positive real root, one negative real root and eight complex roots in our problem domain ($1 < \mathrm{Ra} < 10^{7}$). Thus, the positive real root is selected as the laminarization transition Reynolds number for the Kaupas et al.correlation.

The estimated transition boundaries using the above relations are plotted in Figure 2-2. It is observed that the Bankston, Tanaka and Kaupas correlations for laminarization transition approximately cover similar ranges. Behzadmehr et al. [2003] results, which are also plotted in Figure 2-2, clearly predict that the flow enters a turbulence transition even at a low Reynolds number of 1000 due to disturbances from the heating. Further heating from the laminar-turbulent transition makes the flow to become laminarized due to the buoyancy and acceleration effects. There is a lack of experimental evidence to assess Behzadmehr's numerical predictions at low Reynolds number, which suggests that further experimental data are needed to prove whether multiple transitional zones exist or not.

Shaded zones in Figure 2-2 are approximate zones that the author thinks as a modified heat transfer regime map for heated upward gas flow. The transition condition to natural convection is also not fully understood yet; thus, the transition zone from the laminarized

turbulent flow to turbulent flow for high Rayleigh numbers is not shown on Figure 2-2.

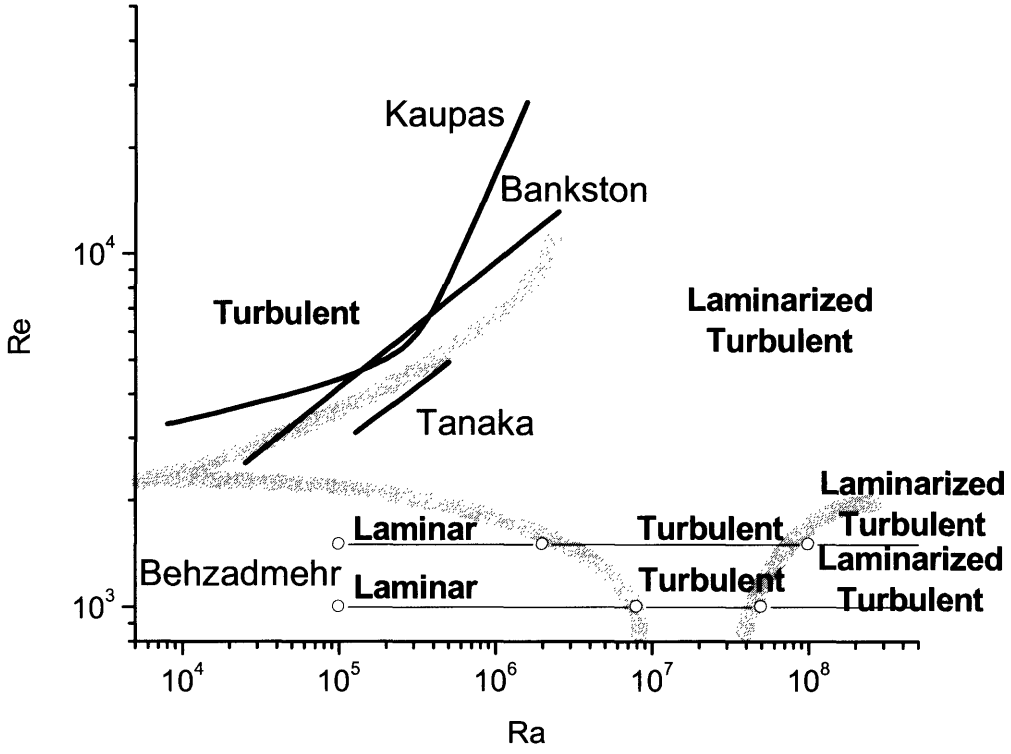

FIGURE 2-2 COMPARISON OF THE TRANSITION CRITERIA

One of the objectives of the experiment designed in this work will be to collect data that can show multiple transitional zones together and demarcate zones clearly in terms of appropriate non-dimensional numbers. This will be explained in more detail in the next chapter.

Table 2-1 is a summary of literature review in this chapter. Most of the works reviewed are sorted in terms of numerical analysis vs. experiment and liquid vs. gas for different flow regimes.

TABLE 2-1 SUMMARY OF LITERATURE REVIEW

	Gas		Liquid	
	Numerical Analysis	Experiment	Numerical Analysis	Experiment
Laminar	[Worsøe-schmidt & Leppert, 1965] [Worsøe-schmidt, 1966] [Zeldin & Schmidt, 1972] [Nesreddine et al., 1998]	[Zeldin & Schmidt, 1972]	[Hallman, 1955]	[Hallman, 1961]
Turbulent (Including Laminarized Turbulent)	[Cotton & Jackson, 1990] [Shehata & McEligot, 1998] [Satake et al., 2000] [Mikielewicz et al., 2002] [You et al., 2003] [Xu et al., 2004] [Spall et al., 2004]	[Bankston, 1970] [Steiner, 1971] [Carr et al., 1973] [Poškas et al., 1989, 1993] [Vilemas et al., 1992] [Shehata & McEligot, 1998] [Polyakov & Shindin, 1988]		[Hall & Jackson, 1969] [Parlatan et al., 1996] [Aicher & Martin, 1996] [Celata et al., 1998]
Laminar to Turbulent	[Behzadmehr et al. 2003]		[Herwig & Schäfer, 1992] [Scheele & Greene, 1966] [Chen & Chung, 2003]	[Scheele & Greene, 1966].
Turbulent to Laminarized Turbulent	[Tanaka et al., 1987]	[Bankston, 1970] [Tanaka et al., 1987] [Kaupas et al. 1989]		[Hall & Jackson, 1969] [Parlatan et al., 1996] [Aicher & Martin, 1996] [Celata et al., 1998]

As a summary of this chapter the following observations are made:

1. The laminar mixed convection regime has more numerical analysis results than the experiment data. The only experiment that was reported in the literature was Hallman's [1961] work. Equation 2-1, which was developed by Churchill [1998], can be used for the heat transfer coefficient correlation. However, the correlation should be tested with the laminar gas mixed convection experimental data for validation.

2. Vast amount of works have been done on the mixed convection turbulent and laminarized turbulent regimes. More heat transfer coefficient correlations were developed based on the liquid experiments compared to gas experiments. Gas experiments mostly concentrated on the flow structure study rather than the correlation development. For the heat transfer correlation, Equation 2-4 can be readily applied and it is the most up-to-date correlation. However, Equation 2-4 needs to be tested with the gas experiments before it could be applied to the gas cooled system design. In addition, the friction factor correlation should also be developed for this flow regime.

3. The transition region is still an open area of research, since it is ambiguous how the previous researchers define the transition criteria from laminar to turbulent flow throughout the literature. It is expected that at least two transitional flow regions exist due to the heating. The first transitional regime is where the laminar flow becomes turbulent earlier than for the adiabatic flow case due to the disturbance from the heating. The second transitional regime is the so-called

"laminarized turbulent" where turbulent flow is laminarized due to further heating, which can cause; (1) buoyancy effect near the wall (2) property variation (3) acceleration of the bulk flow - all affecting the laminarization process.

4. MIT experimental facility will try to cover the regimes as much as possible to understand the heat and mass transfer mechanism in mixed convection regime.

3 DESIGN OF THE NEEDED EXPERIMENT

The preceding literature review suggests that there is a need for an experiment to cover several heat transfer regimes in order to verify the existence of multiple transitional zones, along with development of consistent heat transfer coefficient and friction factor correlations. To address this problem an experimental facility has been designed at MIT with support from Idaho National Laboratory (INL). The designed facility is under construction.

3.1 DESCRIPTION OF THE FACILITY

The two objectives of the test facility are (1) to try to include to the largest extent as possible of the operating range of GFR prototype DHR loop developed at MIT and (2) to cover the flow regime map shown in Table 1-1 with the focus on the mixed convection regime [Cochran et al., 2005]. Detailed description and the thermal-hydraulic characteristics of prototypic loop of GFR's DHR system along with the main design features of the test facility are all provided in Cochran et al.'s work [2005].

A schematic diagram of the experimental loop is shown in Figure 3-1. The test section is 2m long and is preceded by approximately 1m of developing length and followed by 4m of a riser section. The test section is designed to be either a 16 mm or 32 mm inner diameter tube. Direct heating is used to achieve approximately axially and azimuthally uniform heat flux. The flow can be induced by either a circulator or by natural circulation. Two hot-wire probes are to be installed in the loop. One is to measure temperature and velocity profiles simultaneously in the test section to provide information on the flow structure. The other is to measure the flow rate in the loop, together with a highly sensitive differential pressure

transducer, since the flow rate is expected to be very small under natural circulation. From this differential pressure transducer, the frictional pressure drop in the test section can also be measured.

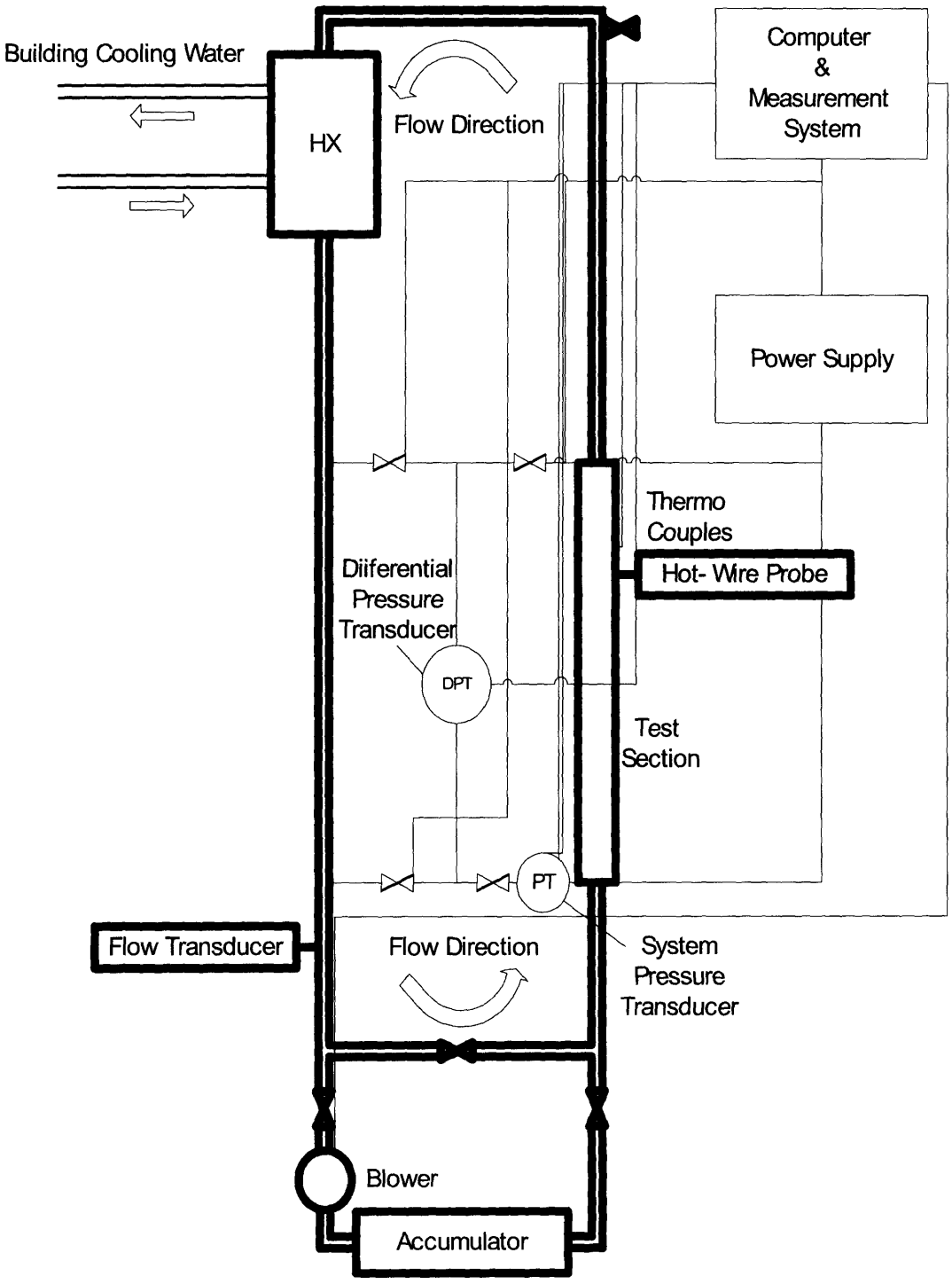

FIGURE 3-1 A SCHEMATIC DIAGRAM OF THE MIT/INL MIXED CONVECTION TEST FACILITY

3.2 PROBE SELECTION AND CALIBRATION

To determine the boundaries between the turbulent and laminar mixed convection, measurement of the radial profile of the velocity and temperature along with the turbulence intensity of the flow are helpful. This is because the mixed convection regime tends to depend on the near wall phenomena such as buoyancy effect, which can be better observed through measuring the profile of the flow rather than just measuring the overall system variables [Shehata & McEligot, 1998]. Also measurements of the velocity and temperature profile can be used to benchmark a Computational Fluid Dynamics (CFD) code such as FLUENT, which helps in developing a model or tool that can analyze the mixed convection regime. In addition, turbulence quantities, such as turbulence intensity, turbulent kinetic energy and so forth, can reveal the flow structure and will aid the understanding of the nature of mixed convection phenomena.

3.2.1 Probe Selection

Since our experiment's final objective is to develop a reasonable correlation for heat transfer coefficient in mixed convection flow regime and fill the gap of past research in this area, it is essential to understand the flow structure itself. Therefore, it is necessary to install a probe that can measure the velocity and temperature profiles across the test section at various flow conditions. A hot-wire, which has been used in many research fields, is going to be utilized for the velocity profile measurement, and the temperature profile will be measured by a cold-wire placed next to the hot-wire.

A hot-wire allows us to measure a velocity component in one position by measuring the

heat that is lost to the flow through cooling. Thus the design characteristics of the probe are; (1) to maintain higher temperature than the surrounding fluid, (2) energy should be supplied from an external circuit, (3) it should be thin enough (approximately 5μm in diameter) to be sensitive to flow velocity variation within a short period of time (lower than 1μs). Since the wire is very vulnerable due to its thinness, a probe component is designed to protect the wire from touching the wall in any case.

The cold-wire measures the temperature profile across the test section by sensing the change in the cold-wire's resistance with the temperature variation of the surrounding fluid. Thus the wire is very thin in order to respond quickly to the flow temperature fluctuation but it does not need to be maintained at a higher temperature like the hot-wire.

There are various configurations of hot-wire anemometers in order to serve different purposes. For our experiment, two different hot-wire probes were considered. Single wire which can measure only one velocity component and a cross wire which can measure two velocity components at the same time. A three-wire probe was not considered from the beginning because we were not interested in measuring three dimensional velocity components, since the azimuthal velocity component can be neglected in a uniformly heated pipe flow. Also, the three-wired probe, due to its size, performs poorly in terms of getting close to the test section wall, where most of the important phenomena would be occurring.

Since a customized cross wire probe is much more difficult to manufacture than a customized single wire probe and the single wire perturbs the flow less than the cross wire does, the cross wire probe was not our first choice. However, to measure two velocity

components with a single hot-wire, an additional control system to rotate the probe is needed.

Both the hot-wire and the cold-wire have been procured from DANTEC Dynamics [http://www.dantecdynamics.com] with customized features and National Instruments is the main provider of the data acquisition system.

3.2.2 Calibration Method

Since resistivity of the hot-wire changes with temperature of the surrounding fluid, the response of the hot-wire varies with temperature. Also, due to non-linearity of the response of hot-wire to the flow velocity, it is necessary to calibrate the probe under the expected experimental conditions of velocity and temperature before going into the actual test facility.

According to Van Dijk and Nieuwstadt [2004], there are many ways to calibrate a hot-wire anemometer, and from the conclusion of the reference the most accurate calibration method is the lookup-table method. The Lookup-table method involves collection of a large amount of data during the calibration phase, generation of a matrix that has temperature dependence of the response and interpolation between the matrix components during the actual measurement. However, this indicates that accurate temperature measurement is an important condition for accurate calibration and measurement of the velocity in the actual experiment. Therefore, the cold-wire should be placed next to the hot-wire to provide the fluid temperature as close to the hot-wire as possible. However, it should be noted that since the hot-wire maintains a higher temperature than the surrounding fluid, radiation and

convection heat transfer from the hot-wire to the cold-wire may cause a problem. This will be solved by calibrating the cold-wire in a facility with the hot-wire and correlating the relationship between those two. Also the radiation effect of the hot-wire itself to the surroundings is another factor that should be considered during the calibration phase, because the radiation effect will be different in the calibration facility and the test section if the geometry is different.

A lookup-table method was not used in the past due to insufficient computational power, even though it has some advantages over other methods. Most of the past researches who used hot-wire did the calibration based on King's Law (Eq. 3-1) with a slight variation of their own, [e.g., Poskas et al., 1993; Meyer, 1992; Koppius & Trines, 1998; Papadopoulos et al. 1999].

$$E^2 = A + BV_{eff}^n \quad \text{(King's Law)} \tag{3-1}$$

E : Electrical Signal of Hot-wire; V_{eff} : Effective Cooling Velocity; A, B, n : Constants

Since n is usually taken as 0.5, Equation 3-1 clearly shows that the velocity holds a non-linear relationship with the hot-wire response. Therefore, linear interpolation within the matrix components may cause some errors. To reduce the error, calibration conditions should employ very fine matrix, where the difference in conditions between two adjacent matrix elements is small. Alternatively, one can use non-linear interpolation scheme in the matrix, which would yield almost the same accuracy as the fine mesh matrix. In our experiment, Equation 3-1 is planned to be used for the interpolation scheme with moderately fine test condition matrix to achieve the minimum error as much as possible. Figure 3-2 shows the flowchart of the calibration scheme

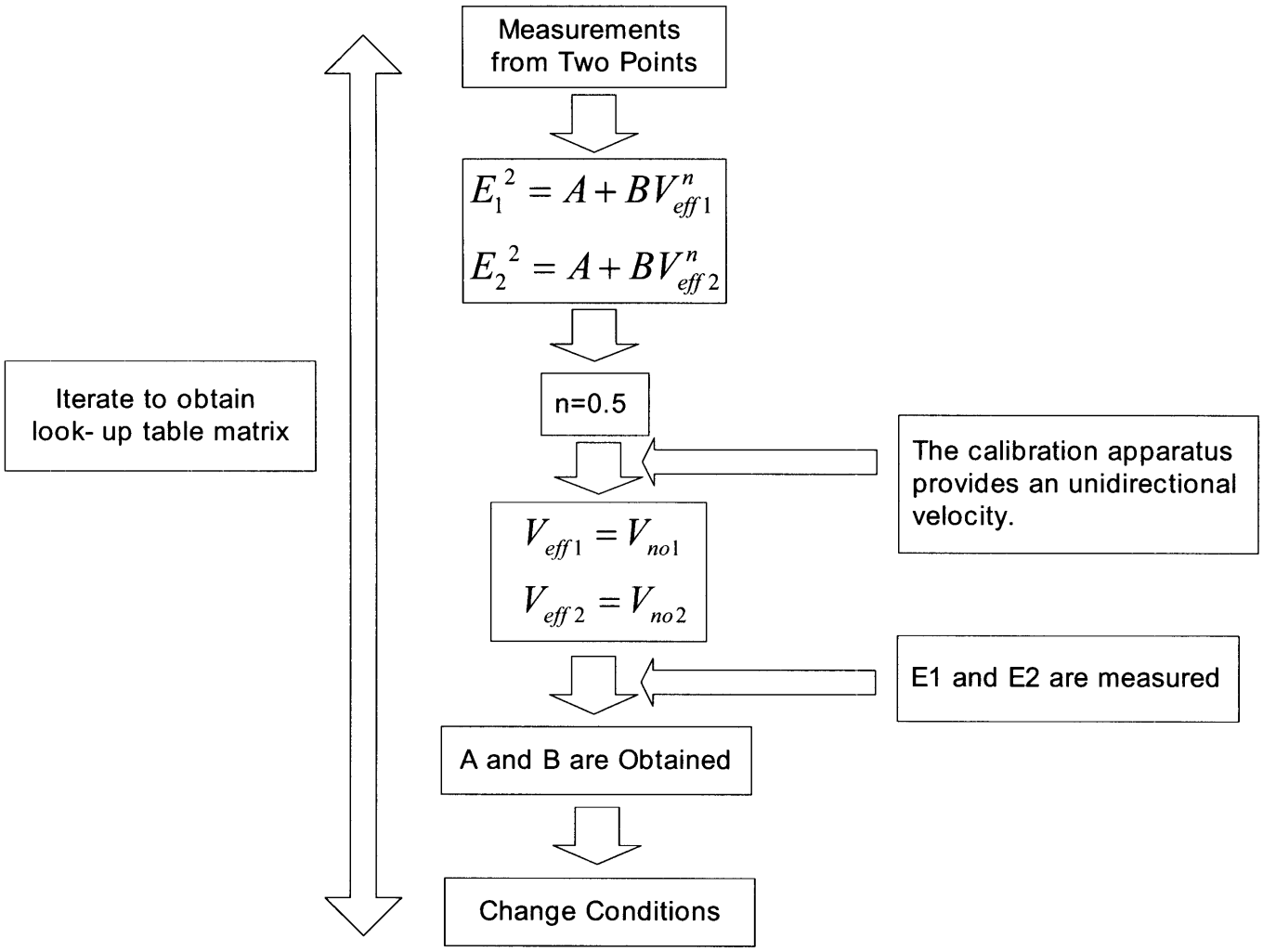

FIGURE 3-2 FLOWCHART OF CALIBRATION SCHEME

As shown in Figure 3-3, arbitrary flow velocity can be viewed as a superposition of three velocity components: Normal, Tangential and Binormal velocity. By these three components, V_{eff} can be expressed as Eq.3-2, taken from the work of Van Dijk [2004].

$$V_{eff}^2 = V_{no}^2 + k_J^2 V_{ta}^2 + h_J^2 V_{bi}^2 \quad \text{(Jorgensen's Law)} \qquad (3\text{-}2)$$

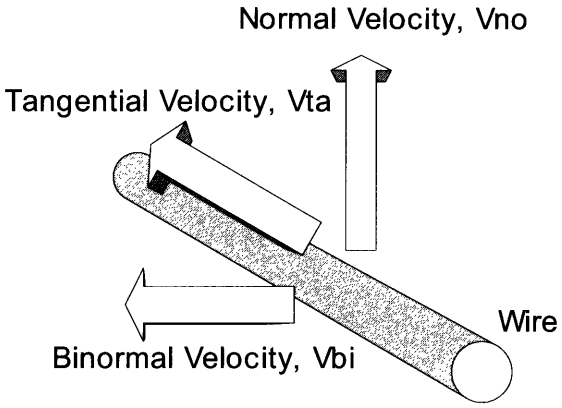

FIGURE 3-3 VELOCITY COMPONENTS AT A HOT-WIRE

The effective cooling velocity is not equivalent to the actual flow velocity. Effective cooling velocity is what the hot-wire senses as the actual flow velocity. Thus conversion from the effective cooling velocity to the actual velocity is needed and it is done by determining the coefficients k_J and h_J during the calibration phase.

Figure 3-4 shows three components of a velocity vector for different positions in laboratory coordinates based on cylindrical coordinates and coordinate attached to the hot-wire that moves along with it. Equation 3-3 is Jorgensen's law applied to two positions in Figure 3-4. Since the azimuthal velocity (V_{ta1} and V_{no2} in Equation 3-3) can be neglected in a uniformly heated gas flow, Equation 3-3 can be rewritten as Equation 3-4.

$$V_{eff1}^2 = V_{no1}^2 + k_J{}^2 V_{ta1}^2 + h_J{}^2 V_{bi1}^2, \quad V_{eff2}^2 = V_{no2}^2 + k_J{}^2 V_{ta2}^2 + h_J{}^2 V_{bi2}^2 \tag{3-3}$$

$$V_{eff1}^2 = V_{no1}^2 + h_J{}^2 V_{bi1}^2, \quad V_{eff2}^2 = k_J{}^2 V_{ta2}^2 + h_J{}^2 V_{bi2}^2 \tag{3-4}$$

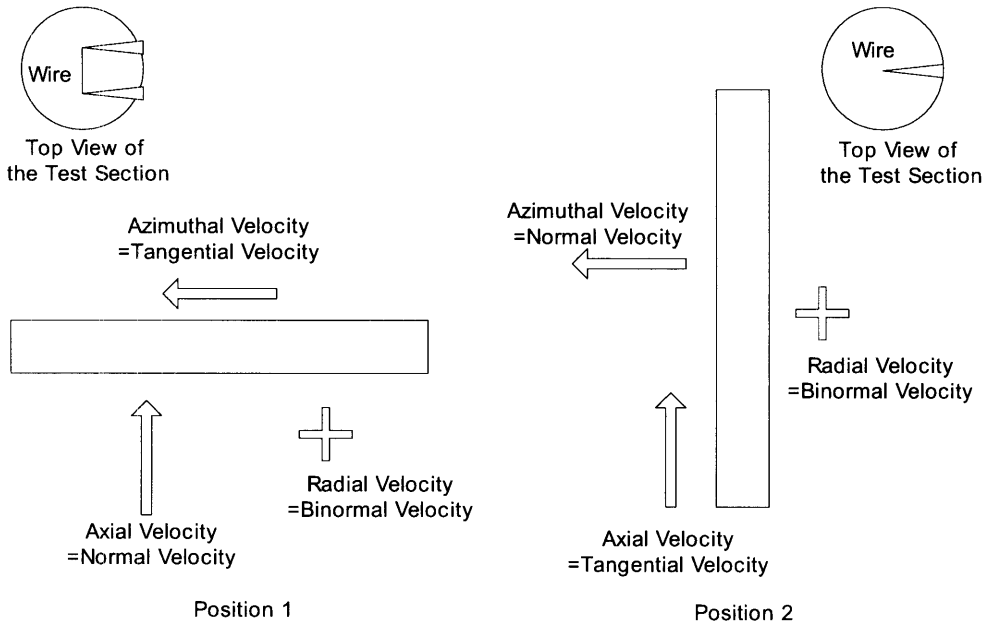

FIGURE 3-4 LAB COORDINATE VS. HOT-WIRE COORDINATE

The coefficients k_j and h_j will maintain the same value for two positions if the surrounding thermodynamical conditions are the same in both positions. Therefore the axial velocity and the radial velocity can be derived from Equation 3-4 if the effective cooling velocity is measured at both positions. Effective cooling velocity is obtained from Equation 3-5 which is King's law applied to two different positions.

$$E_1^2 = A + BV_{eff1}^n, \quad E_2^2 = A + BV_{eff2}^n \tag{3-5}$$

According to van Dijk et al. [2004], n can usually be taken as 0.5. A and B are determined from the two adjacent points in the calibration matrix. These coefficients will also be used for interpolation within the matrix during the actual measurement. It is shown in Figure 3-5 that with appropriate calibration, the procedure will yield a mathematically closed set of equations and promises reasonable accuracy of the measurement.

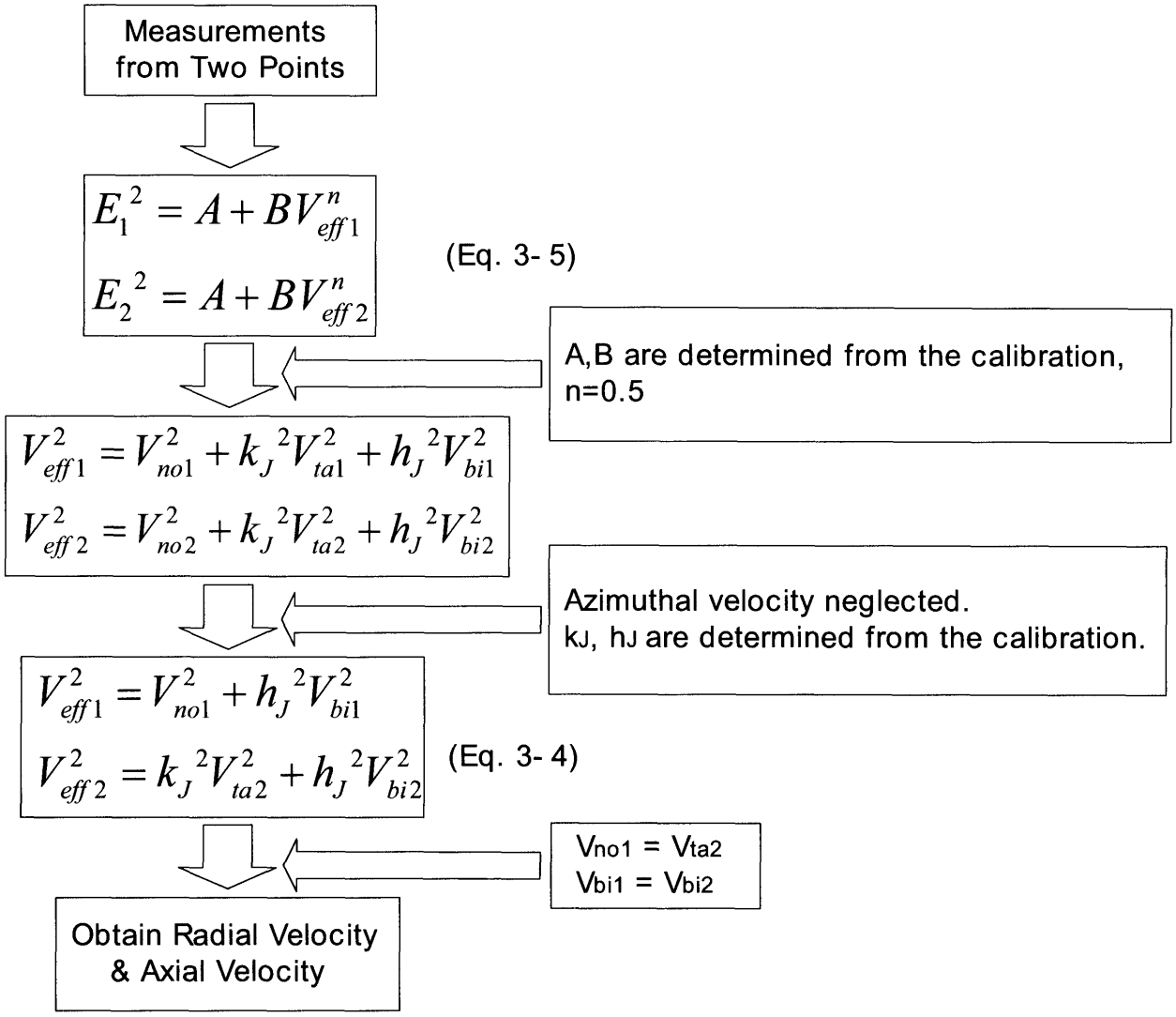

FIGURE 3-5 FLOWCHART FOR OBTAINING VELOCITY FROM A HOT-WIRE SIGNAL IN A LOOP

3.2.3 Calibration facility

A calibration facility requires generating a stream of gas with a known velocity under similar boundary conditions as in the actual experiment. Since our experimental conditions are high temperature with low velocity in a pressurized system, most of the previous calibration facilities, which were usually designed for lower temperature with higher

velocity at atmospheric pressure, are not appropriate for the purpose. Thus designing and building a calibration facility that can fulfill our requirement is another task to be accomplished. To design and build the appropriate apparatus, the calibration facilities of previous workers, such as Van Dijk and Nieuwstadt [2004], Meyer [1992], Koppius and Trines [1998], Papadopoulos et al. [1999] and Shehata [1984], were reviewed to sort out the basic design features that can be useful to our facility design.

The calibration facility should be able to:

i. Provide a gas flow with a known velocity.

ii. Withstand pressure up to 1.0MPa.

iii. Generate high temperature (500℃) gas flow.

iv. Prevent any event that can break the hot-wire sensor.

Figure 3-6 shows the conceptual design of the calibration facility. The heater is needed to heat up the gas to 500℃, the heat exchanger is needed to cool the gas and the blower and the tank will be the same that are used in the main test facility. All the measurement systems are omitted in the figure for simplification. The measurement system will be equipped for measurement of the pressure, temperature and flow rate. Another key feature of the calibration facility is that the facility is attached to the main loop in order to minimize the chances for an event that can break the hot-wire sensor.

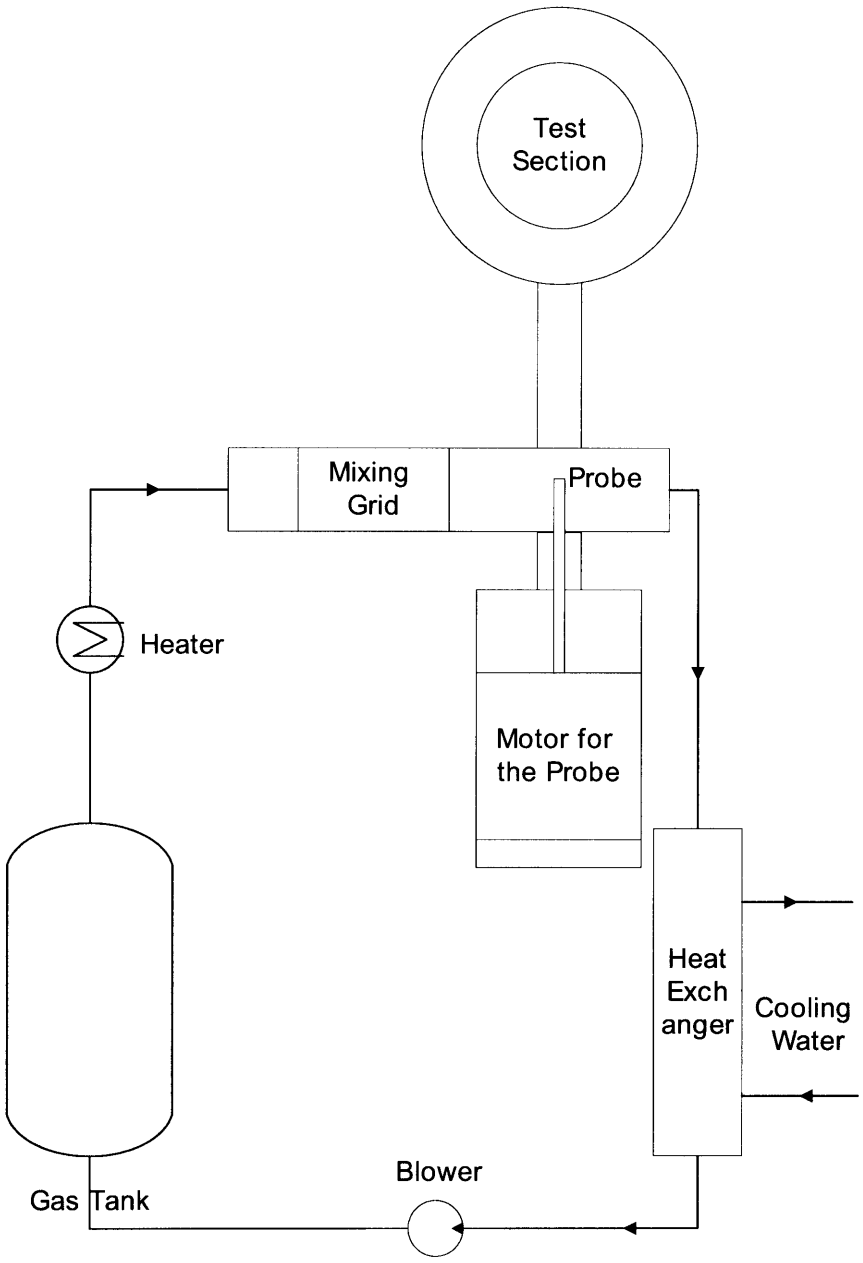

FIGURE 3-6 SCHEMATIC DIAGRAM OF A COMPLETE CALIBRATION FACILITY

Since the author had no experience in the hot-wire sensor operation it was reasonable to build a simple calibration facility first and accumulate preliminary knowledge on the topic to be used to develop and build the final version. Therefore, an experimental apparatus with no heating, which operates at atmospheric pressure using compressed air supply was designed and built. Figure 3-7 shows the detailed view of the test facility and Appendix A shows the photos of each component. The flow meter and static mixer is an OMEGA

product and the other fittings are from McMASTER. The flow meter can measure the velocity up to 2.5 m/s, which is similar to the maximum velocity in the main loop when the flow is generated by natural circulation only. A honeycomb is installed in the flow straightener to straighten the flow and lower the turbulent fluctuation. The test section of this facility utilizes three quarter inch tube, which has exactly the same dimension as the 16mm inner diameter test section of the main loop.

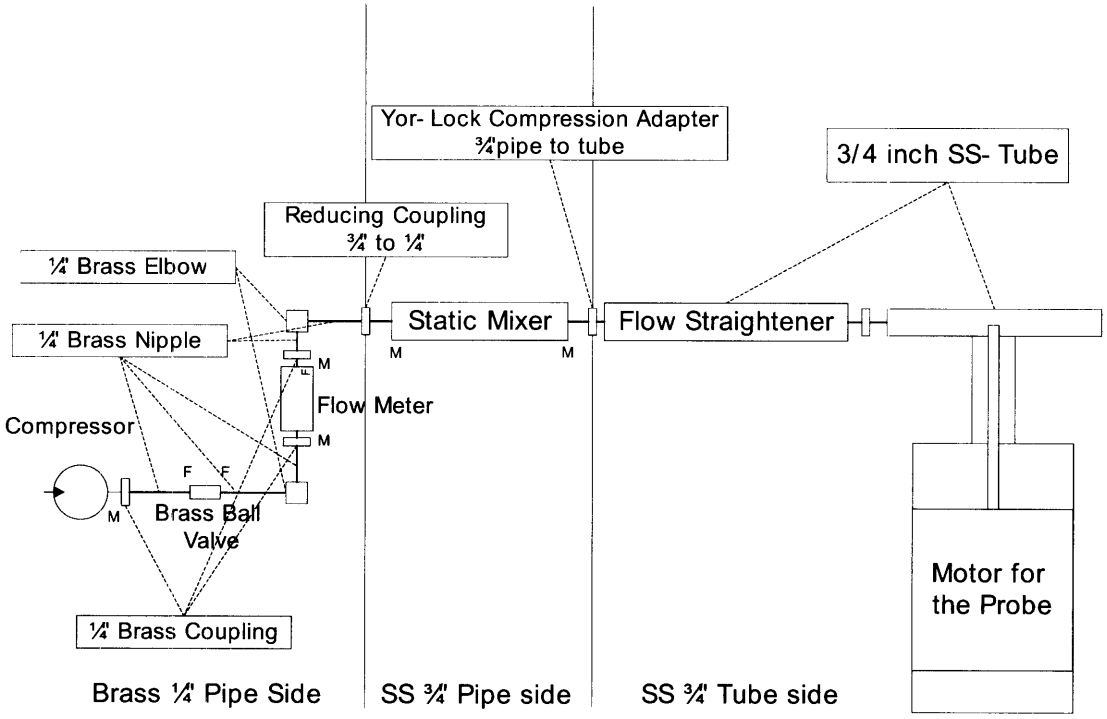

FIGURE 3-7 HOT-WIRE CALIBRATION FACILITY WITHOUT HEATING

The objectives of this facility are to:

i. Determine if the combination of the flow straightener and static mixer is capable of generating a flat velocity profile with a low turbulent fluctuation.

ii. See if the viscous sublayer was small enough in order to integrate the velocity profile to get the flow rate within a reasonable accuracy so as to correlate the hot-wire's electrical signal to the area-average gas velocity

iii. Observe the sensitivity of the hot-wire with the change of orientation.

iv. Develop a preliminary data acquisition system and calibration software for the hot-wire measurement system.

v. Accumulate knowledge on the hot-wire operation before designing the final calibration facility.

Figure 3-8 shows the hot-wire response profile across the test section in the calibration facility for different Reynolds number flow. Figure 3-9 shows the variance of the measured signal. The measurements that are presented in the figures are taken for 2 seconds for each position in the test section. Thus, each point in Figure 3-8 shows the average of the hot-wire signal for 2 seconds at one position and each point in Figure 3-8 shows the variance of the signal for 2 seconds at each position.

It is clearly seen from Figure 3-8 that as Reynolds number decreases the viscous sublayer thickness, denoted as δ, is getting larger, since the flow is becoming more laminar. Also, it is observed that when there is no flow (Re 000 case) there is a large fluctuation in the signal. This is due to the natural convection effect of the hot-wire itself, since the hot-wire has a higher temperature than the ambient temperature. Similar reasoning can explain the trend in Figure 3-9. There is a large fluctuation in the no flow case due to the natural convection instability and relatively high fluctuation at high Reynolds numbers due to turbulence and the fluctuation tend to decay as the Reynolds number decreases since the flow is getting closer to laminar.

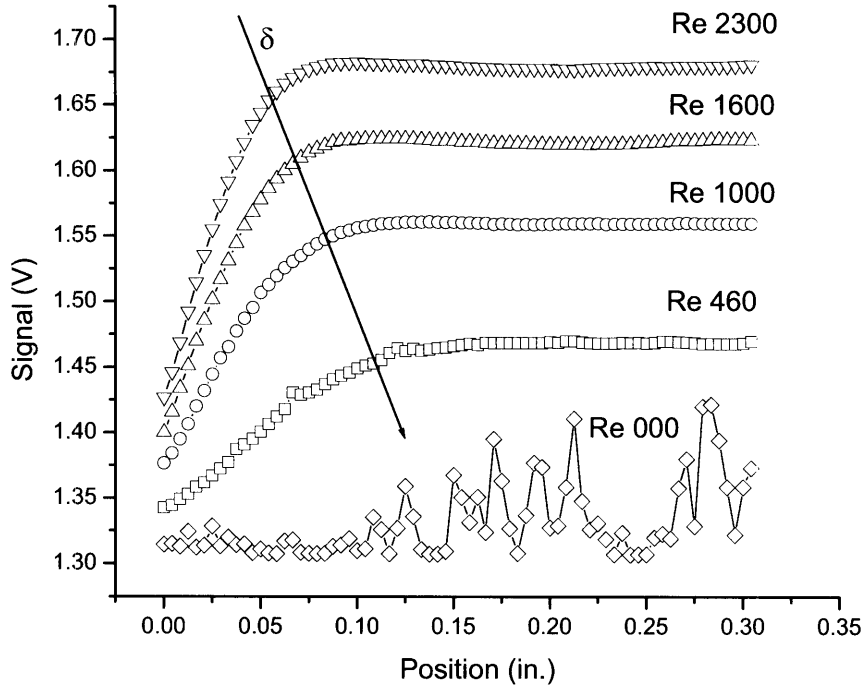

FIGURE 3-8 HOT-WIRE MEASUREMENT FOR DIFFERENT REYNOLDS NUMBER

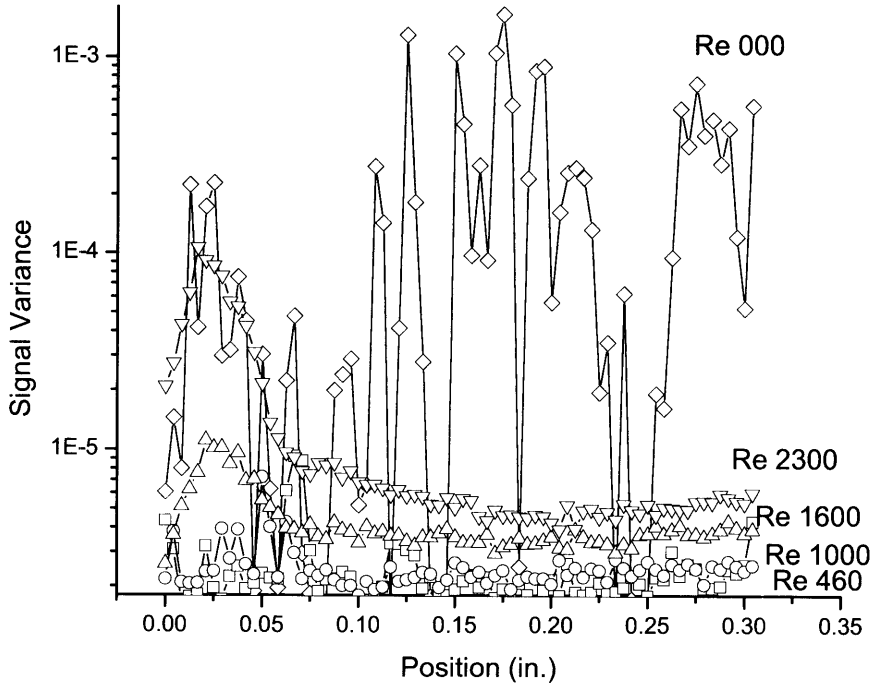

FIGURE 3-9 VARIANCE OF HOT-WIRE SIGNAL FOR DIFFERENT REYNOLDS NUMBER

Since the local velocity of the gas flow and the electrical signal of the hot-wire are not linearly correlated, which can be easily observed from Equation 3-5, it is hard to know the absolute value of velocity at a local position. Also from Figure 3-8, since the viscous sublayer covers a significant flow area, it is not reasonable to ignore the sublayer and integrate to get the average velocity. Therefore, in order to correlate the electrical signal of the hot-wire to the local velocity, it is necessary to measure an absolute velocity by other means, such as a Pitot tube.

Figure 3-10 is a schematic diagram of the Pitot tube that is going to be designed and manufactured for the testing. The mechanism of the Pitot tube is by measuring the difference between the stagnant pressure and the static pressure, the local velocity can be calculated through the Bernoulli's equation. Since, gas has a low density and the operation velocity range of the facility is small, the differential pressure is on the order of Pascal, which is very small. To measure such a low-pressure difference, high precision differential pressure transducer is needed. Thus, the main loop differential pressure transducer, which is used for measuring the friction pressure drop, will be used again for the calibration of the hot-wire, since it has maximum resolution (on the order of less than a Pascal).

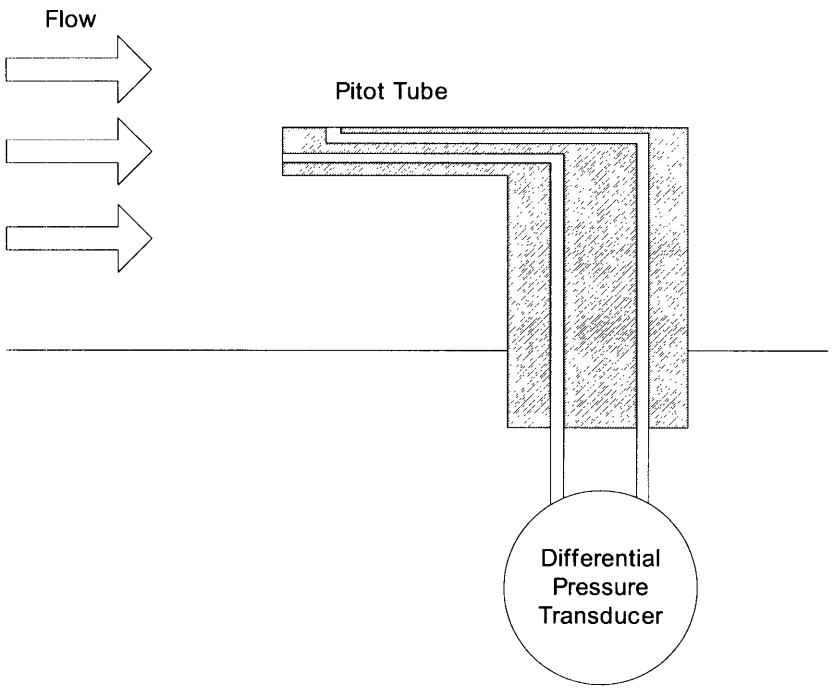

FIGURE 3-10 A SCHEMATIC DIAGRAM OF THE PITOT TUBE

3.2.4 Measurement Software

Figure 3-11 shows the layout of the measurement software. The software can be divided into three different parts. First part includes the calibration package, second part is the on-line processor that is needed during the experiment and the last part is post-processor for data reduction after the measurements are taken in actual test facility. For the on-line processor, it is essential to design the program as simple as possible so that the computer response time can be minimized in order to lower the dead time of probe's response. The software will be programmed primarily with Visual Basic with assistance of other programming languages.

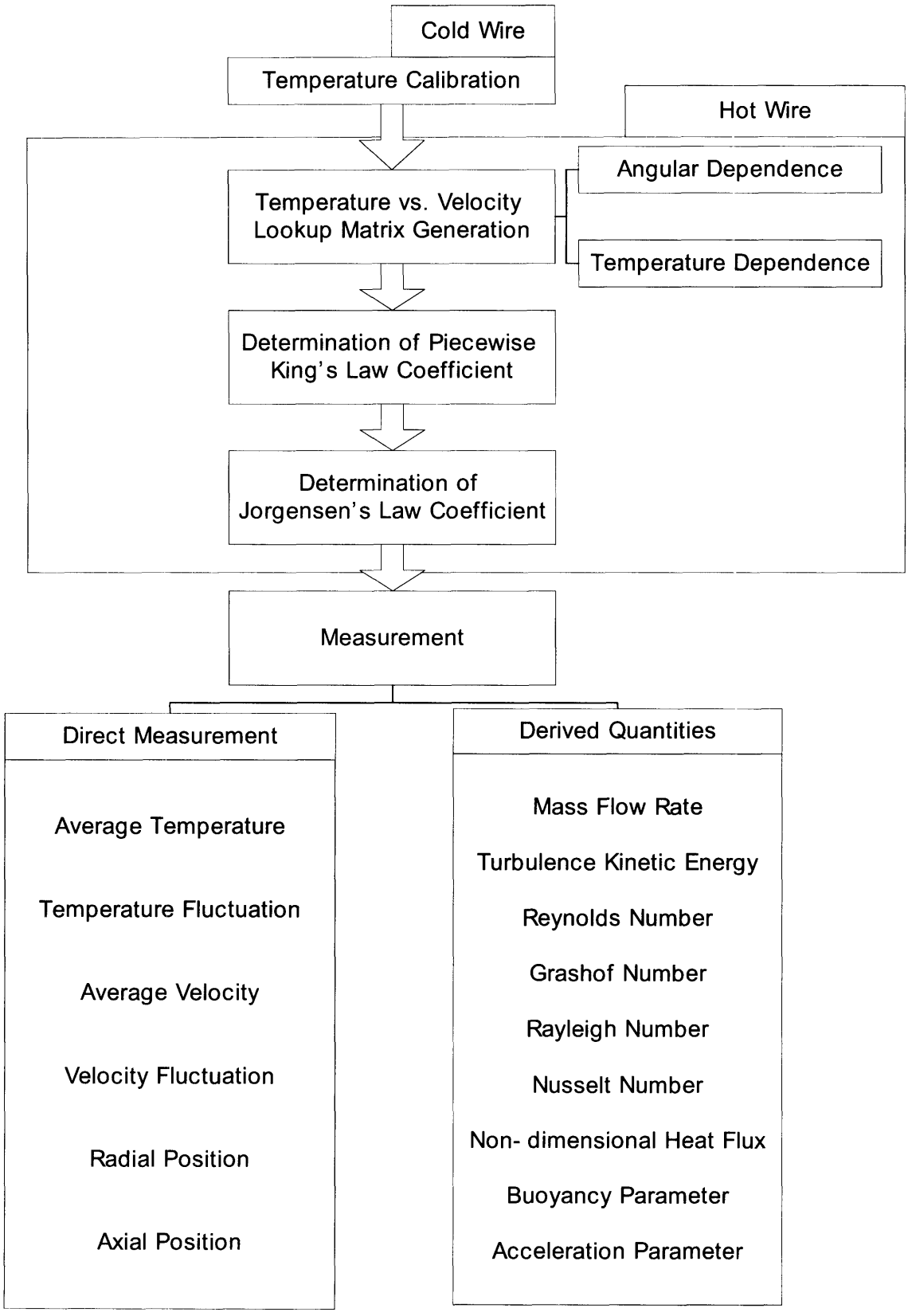

FIGURE 3-11 MEASUREMENT SOFTWARE STRUCTURE

3.3 RANGE COVERED BY THE TEST FACILITY

Figure 3-12 shows the range that can be covered in the MIT experimental facility along with the previous experimental work. The **expected operating conditions** [Cochran et al., 2005] were obtained by using LOCA-COLA code, which was developed at MIT [Williams et al., 2004]. The available experimental data for aiding flow, uniform wall heat flux and gas as an operating fluid are also added on the plot. The experimental data that used a different definition of non-dimensional parameter were all converted to plot on the same Reynolds-Rayleigh flow regime map, by using the same technique that was described in the second chapter and the following Equation.

$$\mathrm{Gr}_q = \frac{g\beta q_w'' D^4}{k\nu^2} = \frac{g\beta\left(T_w - T_b\right)D^3}{\nu^2}\frac{hD}{k} = \mathrm{Gr}_{\Delta T}\mathrm{Nu} \qquad (3\text{-}6)$$

The Nusselt number for the conversion was chosen differently for different sets of data, since most of the data were reported with their own Nusselt number with or without correlation. In the figure, "Kaupas " represents the data from Kaupas and Poškas [1991], which differs from Kaupas et al. [1989]. Earlier work of Kaupas et al. [1989] presented laminarization transition condition without presenting detailed experimental data, so it is excluded from the figure. Also since Kaupas and Poškas [1991] data covers the work of Vilemas et al. [1991], Vilemas et al. data are not separately plotted in Figure 3-12. The legend "Steiner" represents the data of Steiner [1971], "Carr" represents the data of Carr et al. [1973], "Polyakov" represents the data of Polyakov and Shindin [1988] and finally "Shehata" represents the data of Shehata and McEligot [1995].

Figure 3-12 clearly shows that the MIT experimental facility will cover the spectrum of most of the previous work and unexplored region together. Also different gases, namely helium, nitrogen and carbon dioxide will be used, thereby allowing us to achieve wider Reynolds number and Rayleigh number operating ranges compared to the earlier experiments.

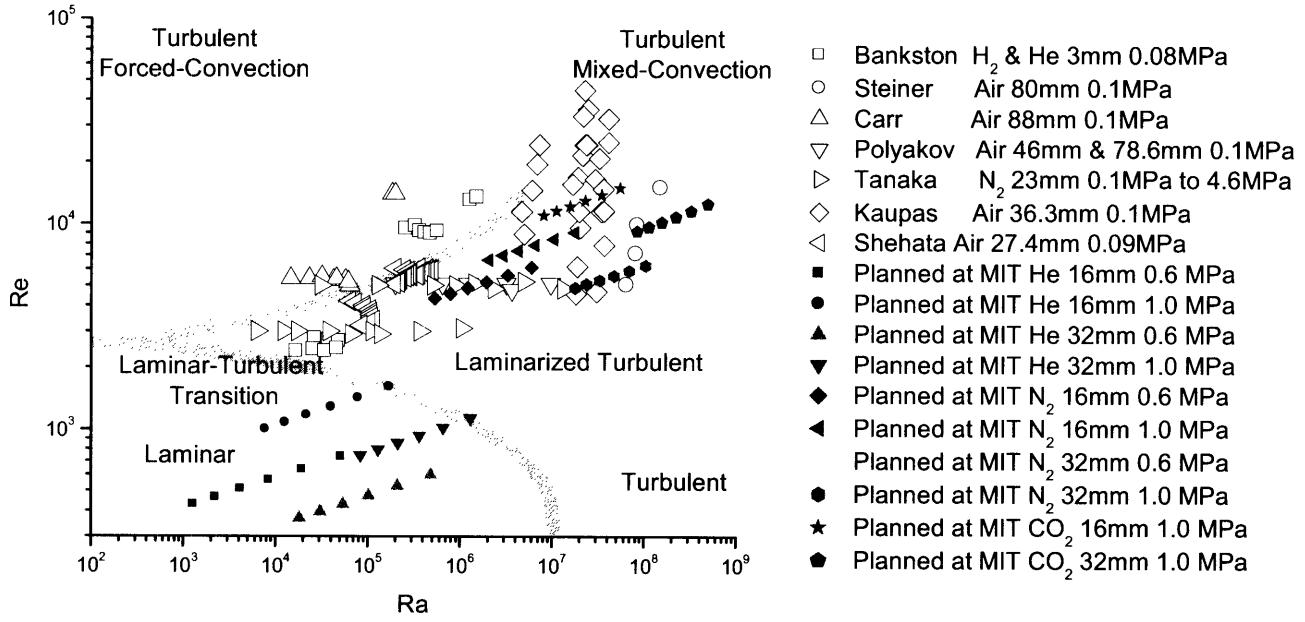

FIGURE 3-12 MIT EXPERIMENTAL FACILITY EXPECTED PERFORMANCE

4 COMPUTATIONAL FLUID DYNAMICS

Most of the turbulence models recognize the onset of transition from laminar to turbulent flow, either by empirical correlations or by other means [Kleiser et al., 1991]. Most of the CFD work on transitional flow is done by DNS or Large Eddy Simulation (LES) [Kleiser et al., 1991]. However, it seems that using the extensive force of computational power to resolve engineering problems such as this one is rarely justified. Thus, for this particular problem, the Behzadmehr et al. [2003] approach is taken, which utilizes a turbulence model to search for multiple transitional zones by observing the behavior of turbulence indicators, such as a turbulent kinetic energy.

It is well known that there is no universal turbulence model that can be applied to all problems. For example, from the work of Satake et al. [2000], Mikielewicz et al. [2002], Xu et al. [2004] and Spall et al. [2004], it can be readily seen that the best fitting model for the measured data of Shehata and McEligot [1995] is still being debated. The author used the commercial CFD code FLUENT to evaluate the performance of selected turbulence models available in this code in the transitional flow region. The models were tested against the data of Shehata and McEligot [1995] and laminar flow calculations at the same time to see if a particular model has the potential to demarcate the transitional zones, following the Behzadmehr et al. [2003] approach. The purpose of this section is only to select an appropriate turbulence model to be compared to the experimental data that will be obtained in the near future at the MIT facility.

FLUENT is able to employ the following models: Spalart-Allmaras (S-A) [1992], k-ε Standard [Launder & Spalding, 1972], k- ε RNG with low Reynolds number formulation [Choudhury, 1993], k- ε Realizable [Shih et al., 1995], k-ω [Wilcox, 1998], Reynolds

Stress Model (RSM) [Gibson & Launder, 1978; Launder, 1989; Launder et al., 1975] and LES with various options to modify each model. LES was ruled out, since it requires a long calculation time with large computational power. Therefore, S-A, k-ω, RSM and three k-εmodels have been tested. A detailed description of each turbulence model can be found in FLUENT user manual [FLUENT, 2001].

The usual procedure of demarcating transition between laminar and turbulent flow is based on the sudden jump in wall shear stress or heat transfer. However, since we are following Behzadmehr's approach, the models were screened by comparison of calculated results to the experimental non-dimensional velocity profile given by Shehata and McEligot [1995] for Reynolds numbers of 4180 and 6030 for adiabatic flow, which is more stringent compared to the usual procedure. Then the sensitivity of the results to mesh size was evaluated. Finally, a laminar flow calculation without heating was performed for the selected models and compared to the Launder-Sharma (L-S) model, which was verified and used by Behzadmehr et al. [2003].

4.1 LOW REYNOLDS NUMBER TURBULENCE CALCULATION

A computer model using FLUENT was built to represent the experimental facility of Shehata and McEligot [1995] as close as possible. The pipe diameter is 27.4 mm and the length of the test section is 32 times of the diameter (32D), which is preceded by 50D hydrodynamical developing length. The test section is followed by 15D calming length, which is not in the experiment but included in order to enhance numerical predictions. The Reynolds number at 4180 was first tested with normal air at atmospheric pressure with no heating. The flow becomes fully-developed in the developing section before entering the test section. All the calculated velocity profiles are taken at 3D downstream from the entrance of the heated test section to match Shehata and McEligot [1995] measurement position.

Figure 4-1 shows that S-A and k-ω models perform much better than the other turbulence models when compared to the measurements of Shehata and McEligot [1995]. Unexpectedly, the k-ε RNG model showed a relatively large error and different trend from the measurements, even though it claims to have a capability of correctly predicting low Reynolds number flow, similar to that of the S-A and k-ω models. The reasons behind the differences among various turbulent model predictions are left as a future work for now.

To check the model capability of simulating higher Reynolds number flow, the S-A and k-ωmodels were tested for Reynolds number of 6030. Figure 4-2 presents the results. Again, both the models agree very well with the measurements of Shehata and McEligot [1995] at higher Reynolds number.

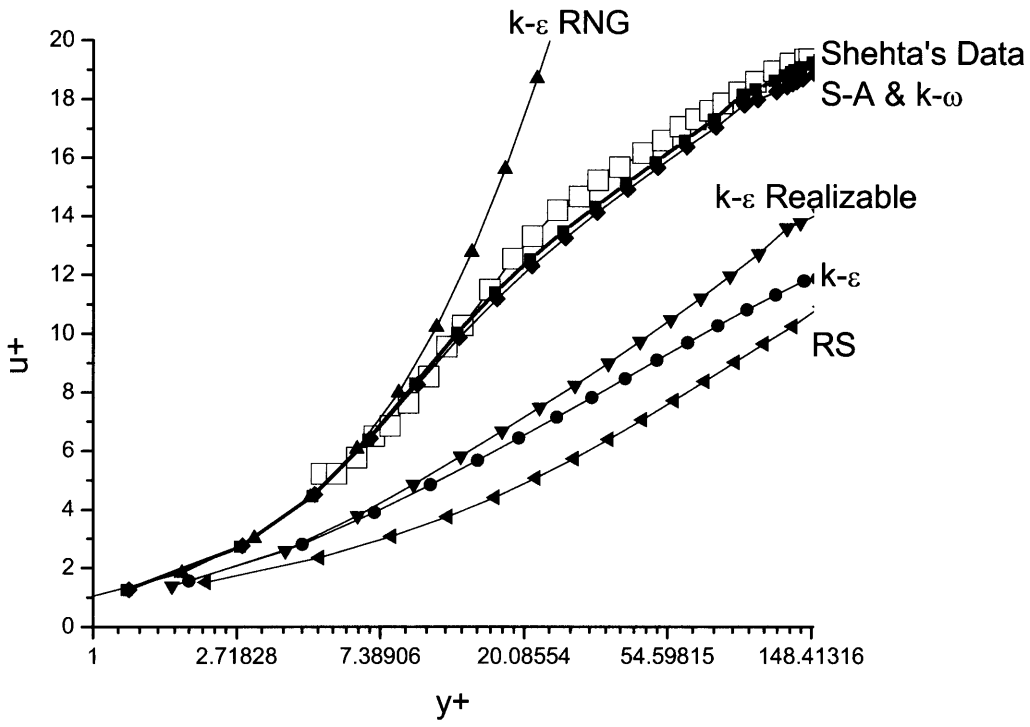

FIGURE 4-1 REYNOLDS NUMBER 4180

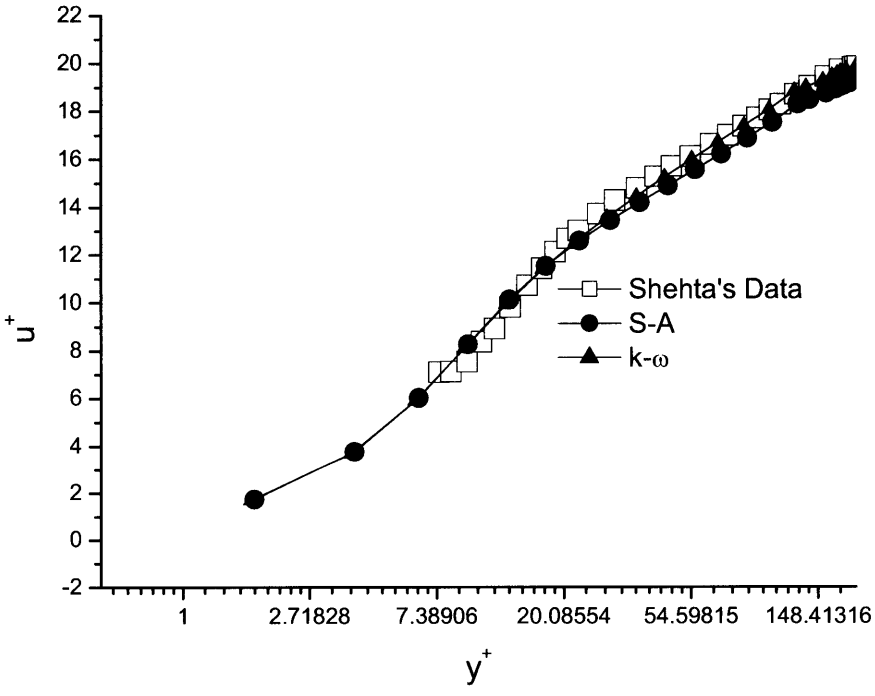

FIGURE 4-2 REYNOLDS NUMBER 6030

4.2 SENSITIVITY TO MESH SIZE

To check if the mesh size used in the above calculations was correctly selected, two grid meshing schemes were compared for the S-A turbulence model with two different Reynolds numbers, 4180 and 6030. The results presented in the preceding section had one quarter million nodes (coarse mesh), while the fine meshing scheme contained approximately three times more nodes than the coarse meshing scheme. Figures 4-3 and 4-4 show that the coarse mesh achieves essentially the same accuracy as the finer meshing calculation. Because coarser mesh achieves the same accuracy at much smaller CPU time, it was selected for future analysis. However, since some models are very sensitive to mesh size below $y^+ = 1$, more extensive studies on the mesh size should be performed in the future.

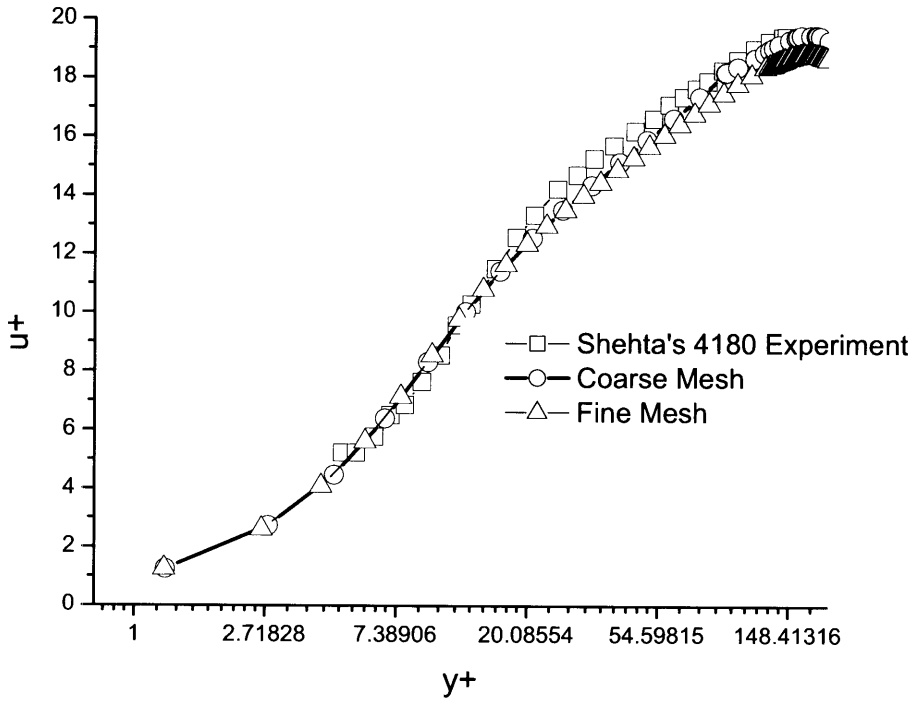

FIGURE 4-3 COMPARISON BETWEEN COARSE MESH AND FINE MESH AT RE=4180

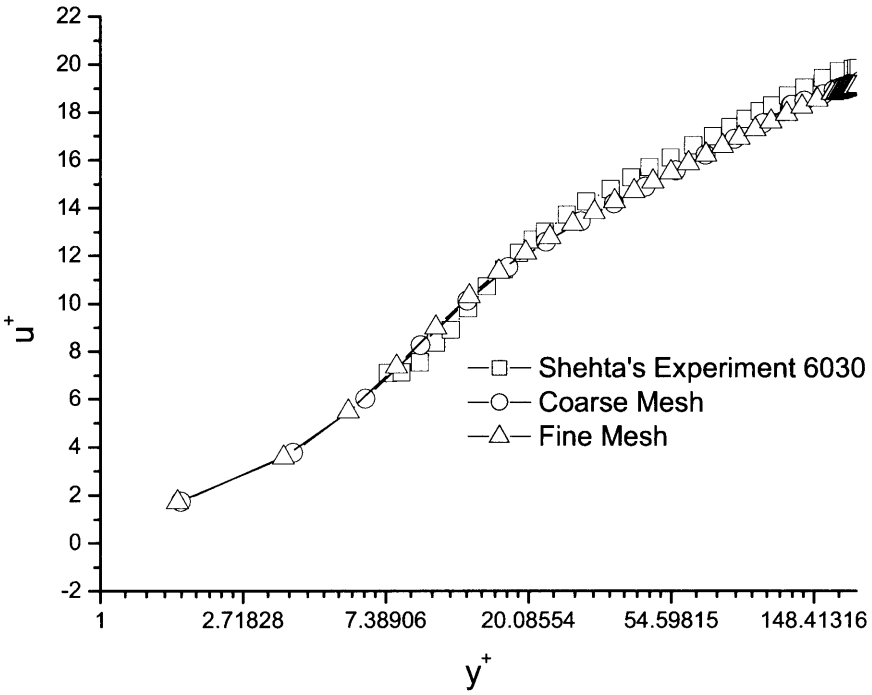

FIGURE 4-4 COMPARISON BETWEEN COARSE MESH AND FINE MESH AT RE=6030

4.3 LAMINAR FLOW CALCULATION COMPARISON

The S-A and k-ω models were tested for fully-developed laminar flow in order to follow Behzadmehr's approach. Since both S-A and k-ω models are for low Reynolds number flow like L-S model is, it was expected to observe similar performance of the S-A, k-ω models with L-S model. A Reynolds number of 1000 was set for the inlet condition with no heating. The velocity profile is compared to the theoretical laminar profile and the L-S model. The L-S model was implemented into FLUENT through the user-defined function (UDF) (See Appendix B).

It can be observed from Figure 4-5 that the S-A and k-ω models perform poorly compared to the L-S model for fully laminar flow. Thus, the basic turbulence models that are implemented in FLUENT package do not perform satisfactorily for finding a transitional zone from laminar to turbulent flow. However, it is possible to implement a turbulence model which is not included in FLUENT package such as the L-S model, by using UDF to utilize an advanced numerical iteration algorithm and post processor features in FLUENT. Thus, for comparing future MIT experimental data in the transitional flow regime, the L-S model should be the first used for benchmarking purposes. Since Spall et al. [2004] concluded that the v^2-f model performs better than the L-S model in certain conditions, the newly implemented v^2-f model in FLUENT should be tested later and compared to the data and the L-S model together.

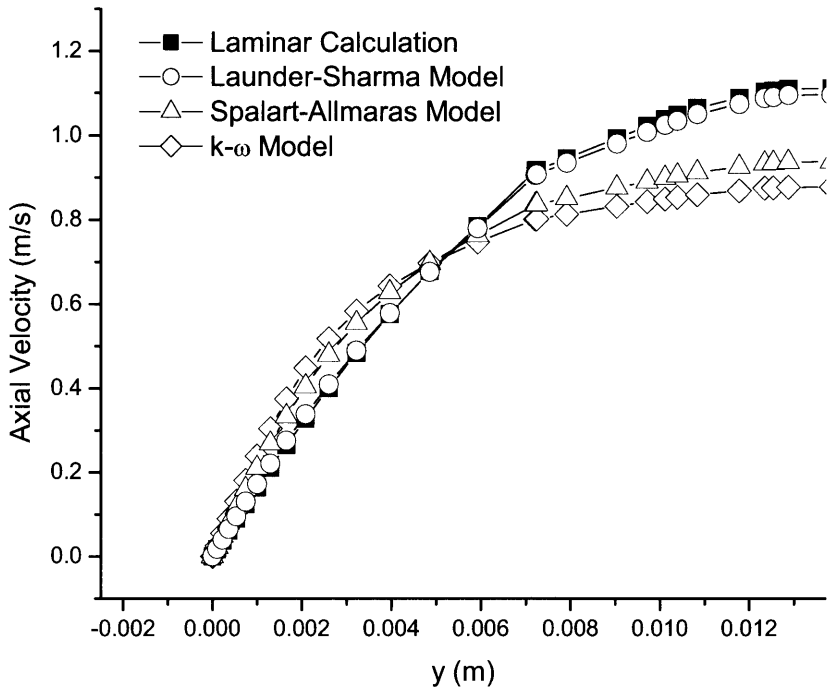

FIGURE 4-5 LAMINAR CALCULATION AT RE=1000 (UNHEATED)

5 CONCLUSION & FUTURE WORK

5.1 CONCLUSIONS

Designers of conceptual GFRs are seriously considering passive DHR systems in order to achieve high standards of safety. However, passive heat removal systems in GFRs are likely to operate in flow regimes not fully understood, such as the mixed convection transitional flow regime.

A literature review of mixed convection thermal and hydraulic characteristics was performed. Although many investigations have been reported on laminar and turbulent mixed convection regimes, there is no agreement on the proper heat transfer and friction factor correlations for a gas-cooled system. Gas flow experiments need to be performed beforehand to validate or generate the proper correlations. This is partly because most of the correlations were developed from liquid flow experiments and the literature review clearly shows that liquid and gas can behave differently when they are heated. Ambiguous points in mixed convection transitional flow regime were identified and the differences between two transitional zones were described. The first transitional zone demarcates the changeover from laminar to turbulent flow. The second transitional zone occurs when additional high heating induces large buoyancy force near the wall and accelerates the bulk flow with a consequence of laminarization and reduced heat transfer coefficient.

An experimental facility is designed in order to determine the transition process and explore the regions not covered by previous work. To understand the flow structure and the mechanisms of flow destabilization and stabilization, it is essential to measure the velocity and temperature profiles and turbulence intensity for different conditions. The well-known

hot-wire technique is applied to measure the profiles in our experiment. Since the accuracy of a hot-wire measurement depends on its calibration, a preliminary calibration apparatus is also designed to accumulate experience before finalizing the calibration facility design. From the experience of the preliminary operation of the calibration apparatus, it is concluded that an independent methodology of measuring the velocity is needed for the calibration purpose. Therefore, a Pitot tube is designed and planned to be installed and tested for applicability to our apparatus.

Numerical analysis was also carried out by applying various turbulence models abailable in the FLUENT commercial CFD code. The analyses were done to determine if the turbulence models have the potential to simulate the transitional mixed convection flow. It was concluded that the basic models in FLUENT were not capable of predicting the transitional flow as the Launder-Sharma turbulence model does, which was shown in Behzadmehr's work and partially proven in this work. Nevertheless, the advanced numerical algorithm and convenient postprocessor of FLUENT can still be utilized by using a User Defined Function capability in FLUENT to incorporate the Launder-Sharma turbulence model and other turbulence models into the code.

5.2 FUTURE WORK RECOMMENDATIONS

As was explained in the literature review, most of the heat transfer correlations for the mixed convection regime were developed from liquid experiments. Since the temperature dependence of the properties of liquids and gases is different, it is reasonable to conclude that for high heating cases, where large temperature gradients are expected across the fluid, liquid and gas may behave differently. Thus the heat transfer correlations for both laminar and turbulent mixed convection need to be examined in gas flow experiments before they are applied to a gas-cooled system design.

The few friction factor correlations for mixed convection regime found in the literature lack thorough measurements and are also mostly inconsistent. From the Reynold's analogy it is well known that friction factor is related to the heat transfer coefficient. Therefore, it is recommended that, to develop a proper heat transfer correlation, the friction factor should also be investigated in the future.

From Spall et al. [2004] work, the v^2-f turbulence model performs better than the Launder-Sharma turbulence model in some cases. Thus the v^2-f turbulence model needs to be verified for applicability to transitional flow prediction. This can be done through FLUENT also, since the recent version of FLUENT6.1 embedded the v^2-f turbulence model.

As a final recommendation for future work, various approaches should be attempted to understand the transition from laminar to turbulent flow, such as describing the maintenance of turbulence through the transport of the vorticity, including the density

fluctuation in the turbulence equation and so on. Since it is not straightforward to observe from the momentum and energy conservation equations itself why heating can stabilizes and destabilizes the flow at certain conditions, more analysis and investigations are needed to provide a clearer picture of the mixed convection regime.

REFERENCES

Aicher T. and Martin H., "New Correlation for Mixed Turbulent Natural and Forced Convection Heat Transfer in Vertical Tubes", International Journal of Heat & Mass Transfer, Vol. 40, No. 15, pp. 3617-3626, 1997

Bankston C. A., "The Transition from Turbulent to Laminar Gas Flow in a Heated Pipe", Journal of Heat Transfer, pp. 569-579, November 1970

Behzadmehr A., Galanis N. and Laneville A., "Low Reynolds Number Mixed Convection in Vertical Tubes with Uniform Wall Heat Flux", International Journal of Heat & Mass Transfer, Vol. 46, pp. 4823-4833, 2003

Carr A. D., Connor M. A. and Buhr H. O., "Velocity, Temperature, and Turbulence Measurements in Air for Pipe Flow with Combined Free and Forced Convection", Journal of Heat Transfer, pp. 445-452, November 1973

Celata Gian Piero, D'Annibale Francesco, Chiaradia Andrea and Cumo Maurizio, "Upflow Turbulent Mixed Convection Heat Transfer in Vertical Pipes", International Journal of Heat & Mass Transfer, Vol. 41, pp. 4037-4054, 1998

Chen Yen-Cho and Chung J. N., "A Direct Numerical Simulation of Transition Phenomena in a Mixed Convection Channel Flow", Computers & Fluids, Vol. 32, pp. 795-822, 2003

Churchill S. W., "Combined Free and Forced Convection in Channels", Heat Exchanger Design Handbook, Chp. 2.5.10, Begell House, Inc., 1998

Choudhury D., Introduction to the Renormalization Group Method and Turbulence Modeling, Fluent Inc. Technical Memorandum TM-107, 1993

Cochran P., Saha P., Hejzlar P., McEligot D. M., McCreery G. E. and Schultz R. R., "Scaling Analysis and Selection of Test Facility for Fundamental Thermal-Hydraulic Studies related to Advanced Gas-Cooled Reactor", *INL/EXT-05-00158*, Idaho National Laboratory and Massachusetts Institute of Technology, Department of Nuclear Science and Engineering, 2005

Cotton M. A. and Jackson J. D., "Vertical Tube Air Flows in the Turbulent Mixed

Convection Regime Calculated Using a Low-Reynolds-Number k-ε Model", International Journal of Heat & Mass Transfer, Vol. 33, No. 2, pp. 275-286, 1990

FLUENT Inc.,"FLUENT 6.0 User's Guide Vol. 2", FLUENT INC., December 2001

Gibson M. M. and Launder B. E., "Ground Effects on Pressure Fluctuations in the Atmospheric Boundary Layer", Journal of Fluid Mechanics, Vol. 86, pp. 491-511, 1978

Hall W. B. and Jackson J. D., "Laminarization of a Turbulent Pipe Flow by Buoyancy Forces", ASME 69-HT-55, 1969

Hallman T. M., "Combined Forced and Free-Laminar Heat Transfer in Vertical Tubes with Uniform Internal Heat Generation", Transaction of American Society of Mechanical Engineers, Vol. 78, pp. 1831-1841, 1955

Hallman T. M., "Experimental Study of Combined Forced and Free Laminar Convection in a Vertical Tube", NASA Technical Note, TN D-1104, December 1961

Hanks Richard W., "The Laminar-Turbulent Transition for Flow in Pipes, Cocentric Annuli, and Parallel Plates", American Institute of Chemical Engineers Journal, Vol. 9, No. 1, pp. 45-48, January 1963

Herwig H. and Schäfer P., "Influence of Variable Properties on the Stability of Two-Dimensional Boundary Layers", Journal of Fluid Mechanics, Vol. 243, pp. 1-14, 1992

Jackson J. D., Cotton M. A. and Axcell B. P., "Studies of Mixed Convection in Vertical Tubes", International Journal of Heat & Fluid Flow, Vol. 10, pp. 2-15, March 1989

Kakaç Sadık, Shah Ramesh K. and Aung Win, "Handbook of Single-Phase Convective Heat Transfer", Chp. 15, John Wiley & Sons, 1987

Kays W. M., Crawford M. E., "Convective Heat and Mass Transfer", 3rd edition, McGraw-Hill, Inc., 1993

Kaupas V. E., Poškas P. S. and Vilemas J. V., "Heat Transfer to a Transition-Range Gas Flow in a Pipe at High Heat Fluxes (2.Heat Transfer in Laminar to Turbulent Flow Transition)", 1989 Scripta Techinca, Inc. pp.340-351, 1989

Kaupas V. E. and Poškas P. S., "Heat Transfer to a Transition-Range Gas Flow in a Pipe at High Heat Fluxes (4.Correlation of Data on Combined (Free and Forced) Convection in the Case of Constant Physical Properties of the Flow)", 1991 Scripta Techinca, Inc. pp.21-37, 1991

Kaupas V. E. and Poškas P. S., "Effect of Variability of the Physical Properties of the Gas on Combined (Free and Forced) Convection Heat Transfer in Vertical Pipes", 1991 Scripta Techinca, Inc. pp.352-365, 1991

Kleiser Leohard and Zang Thomas A., "Numerical Simulation of Transition in Wall-Bounded Shear Flows", Annual Reviews on Fluid Mechanics., Vol. 23, pp. 495-537, 1991

Koppius A. M. and Trines G. R. M., "The dependence of hot-wire calibration on gas temperature at low Reynolds number", International Journal of Heat and Mass Transfer Vol. 19 pp.967-974, 1998

Launder B. E. and Sharma B. I., "Application of the Energy-Dissipation Model of Turbulence to the Calculation of Flow Near a Spinning Disc", Letters in Heat and Mass Transfer, Vol. 1, pp. 131-138, 1974

Launder B. E., Reece G. J., and Rodi W., "Progress in the Development of a Reynolds-Stress Turbulence Closure", Journal of Fluid Mechanics, Vol. 68(3), pp. 537-566, 1975

Launder B. E., "Second-Moment Closure: Present... and Future?", International Journal of Heat Fluid Flow, Vol. 10(4), pp. 282-300, 1989

McEligot D. M. and Coon C. W. and Perkins H. C., "Relaminarization in Tubes", International Journal of Heat & Mass Transfer: Shorter Communications, Vol.13, pp. 431-433, 1969

Metais B. and Eckert E. R. G., "Forced, Mixed and Free Convection Regimes", Journal of Heat Transfer, pp. 295-297, May 1964

Meyer, L., "Calibration of a three-wire probe for measurements in non-isothermal flow", Experimental Thermal and Fluid Science Vol. 5 pp. 260-267, 1992

Mikielewicz Dariusz P., Shehata A. Mohsen, Jackson J. Derek and McEligot Donald M., "Temperature, Velocity and Mean Turbulence Structure in Strongly Heated Internal Gas

Flows Comparison of Numerical Predictions with Data", International Journal of Heat & Mass Transfer, Vol. 45, pp. 4333-4352, 2002

Nesreddine H., Galanis N. and Nguyen C. T., "Effects of Axial Diffusion on Laminar Heat Transfer with Low Peclet Numbers in the Entrance Region of Thin Vertical Tubes", Numerical Heat Transfer, Part A, Vol. 33, pp. 247-266, 1998

Papadopoulos K. H., Soilemes A. T., Helmis C. G. and Papageoragas P. G., "A hot-wire based, research atmospheric turbulence probe: design analysis and performance", Measurement Vol. 25 pp.53-69, 1999

Parlatan Y., Todreas N. E. and Driscoll M. J., "Buoyancy and Property Variation Effects in Turbulent Mixed Convection of Water in Vertical Tubes", Journal of Heat Transfer, Vol. 118, pp. 381-387, May 1996

Petukhov B. S. and Polyakov A. F., "Heat Transfer in Turbulent Mixed Convection", Hemisphere Publishing Corporation, 1988

Polyakov A. F. and Shindin S. A., "Development of Turbulent Heat Transfer over the Length of Vertical Tubes in the Presence of Mixed Air Convection", International Journal of Heat & Mass Transfer, Vol. 31, No. 5, pp. 987-992, 1988

Poškas P. S., Kaupas V. E. and Vilemas J. V., "Heat Transfer to a Transition-Range Gas Flow in a Pipe at High Heat Fluxes (3.Effect of Buoyancy on Local Heat Transfer in Forced Turbulent Flow)", 1989 Scripta Techinca, Inc. pp.352-361, 1989

Poškas P. S., Kaupas V. E. and Pabarčius R., "Average and fluctuating velocity and temperature distribution along a vertical tube with combined convection", Heat and Transfer Research Vol. 25 No. 5, 1992

Poškas P. S., Kaupas V. E. and Pabarčius R., "Average and Fluctuating Velocity and Temperature Distributions Along a Vertical Tube with Combined Convection", 1995 Scripta Techinca, Inc. pp.589-603, 1993

Satake Shin-ichi, Kunugi Tomoaki, Shehata A. Mohsen and McEligot Donald M., "Direct Numerical Simulation for Laminarization of Turbulent Forced Gas Flows in Circular Tubes with Strong Heating", International Journal of Heat and Fluid Flow, Vol. 21, pp. 526-534, 2000

Scheele George F. and Greene Howard L., "Laminar-Turbulent Transition for Nonisothermal Pipe Flow", American Institute of Chemical Engineers Journal, Vol. 12, No. 4, July 1966

Shehata Mohsen A. "Mean Turbulence Structure in strongly heated air flows.", Ph.D. thesis, University of Arizona, 1984

Shehata Mohsen A. and McEligot Donald M., "Turbulence Structure in the Viscous Layer of Strongly Heated Gas Flows", Idaho National Engineering Laboratory Report, INEL-95/0223, 1995

Shehata Mohsen A. and McEligot Donald M., "Mean Structure in the Viscous Layer of Strongly-Heated Internal Gas Flows. Measurements", International Journal of Heat & Mass Transfer, Vol. 41, pp. 4297-4313, 1998

Shih T.-H., Liou W. W., Shabbir A., and Zhu J., "A New k-ε Eddy-Viscosity Model for High Reynolds Number Turbulent Flows - Model Development and Validation", Computers Fluids, Vol. 24(3), pp. 227-238, 1995

Spalart P. and Allmaras S., "A one-equation turbulence model for aerodynamic flows", Technical Report AIAA-92-0439, American Institute of Aeronautics and Astronautics, 1992

Spall Robert E., Richards Adam and McEligot Donald M., "An Assessment of k-ω and v^2-f Turbulence Models for Strongly Heated Internal Gas Flows", Numerical Heat Transfer, Part A, Vol. 46, pp. 831-849, 2004

Steiner Alejandro, "On the Reverse Transition of a Turbulent Flow under the action of Buoyancy Forces", Journal of Fluid Mechanics, Vol. 47 Part 3, pp. 503-512, 1971

Tanaka Hiroaki, Maruyama Shigeo and Hatano Shunichi, "Combined Forced and Natural Convection Heat Transfer for Upward Flow in a Uniformly Heated, Vertical Pipe", International Journal of Heat & Mass Transfer, Vol. 30, No. 1, pp. 165-174, 1987

Wilcox D. C., Turbulence Modeling for CFD, DCW Industries, Inc., La Canada, California, 1998

Van Dijk A. and Nieuwstadt F. T. M., "The calibration of (multi-)hot-wire probes. 2. Velocity-calibration", Experiments in Fluids Vol. 36 pp.550-564, 2004

Vilemas J., Ušpuras E. and Šimonis V., "Turbulent Momentum and Heat Transfer in Channel Gas Flow at High Heat Loads", Experimental Thermal and Fluid Science, Vol. 4, pp. 375-398, 1991

Vilemas J. V., Poškas P. S., and Kaupas V. E., "Local Heat Transfer in a Vertical Gas-Cooled Tube with Turbulent Mixed Convection and Different Heat Fluxes", International Journal of Heat & Mass Transfer, Vol. 35, No. 10, pp. 2421-2428, 1992

Williams W. C., Hejzlar P. and Driscoll M. J., "Decay Heat Removal from GFR Core by Natural Convection", International Congress on Advances in Nuclear Power Plants ICAPP '04, Paper 4166, Pittsburgh, USA, June 13-17, 2004

Worsøe-schmidt P. M. and Leppert G., "Heat Transfer and Friction for Laminar Flow of Gas in a Circular Tube at High Heating Rate", International Journal of Heat & Mass Transfer, Vol. 8, pp. 1281-1301, 1965

Worsøe-schmidt P. M., "Heat Transfer and Friction for Laminar Flow of Helium and Carbon Dioxide in a Circular Tube at High Heating Rate", International Journal of Heat & Mass Transfer, Vol. 9, pp. 1291-1295, 1966

Xu Xiaofeng, Lee Joon Sang, Pletcher Richard H., Shehata A. Mohsen and McEligot Donald M., "Large Eddy Simulation of Turbulent Forced Gas Flows in Vertical Pipes with High Heat Transfer Rates", International Journal of Heat & Mass Transfer, Vol. 47, pp. 4113-4123, 2004

Yan W. M. and Lin T. F., "Theoretical and Experimental Study of Natural Convection Pipe Flows at High Rayleigh Number", International Journal of Heat & Mass Transfer, Vol. 34, No.1, pp. 291-303, 1991

You Jongwoo, Yoo Jung Y. and Choi Haecheon, "Direct Numerical Simulation of Heated Vertical Air Flows in Fully Developed Turbulent Mixed Convection", International Journal of Heat & Mass Transfer, Vol. 46, pp. 1613-1627, 2003

Zeldin B. and Schmidt F. W., "Developing Flow with Combined Forced-Free Convection in an Isothermal Vertical Tube", Journal of Heat Transfer, pp. 211-223, May 1972

APPENDIX A : PHTOGRAPHS OF CALIBRATION APPARATUS

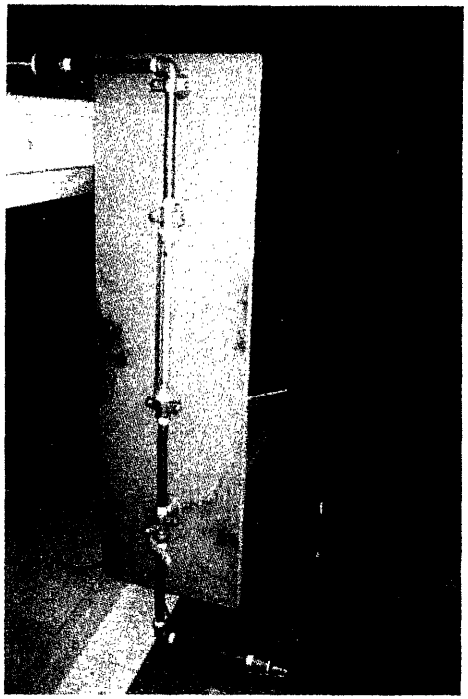

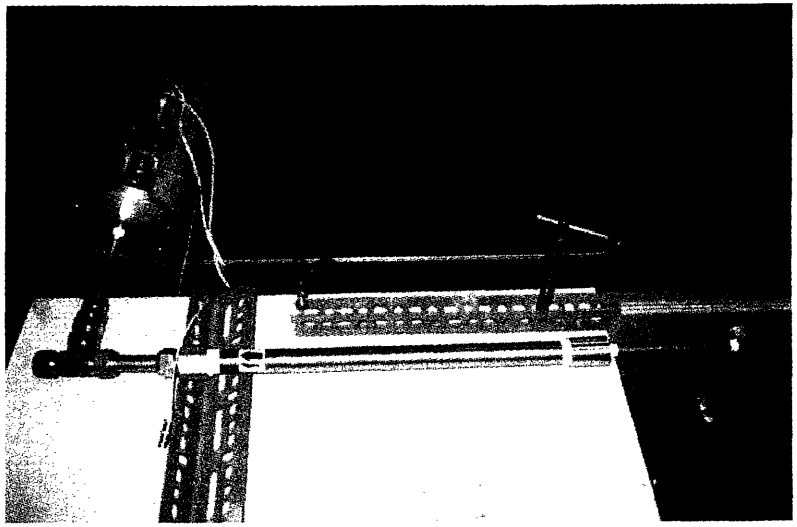

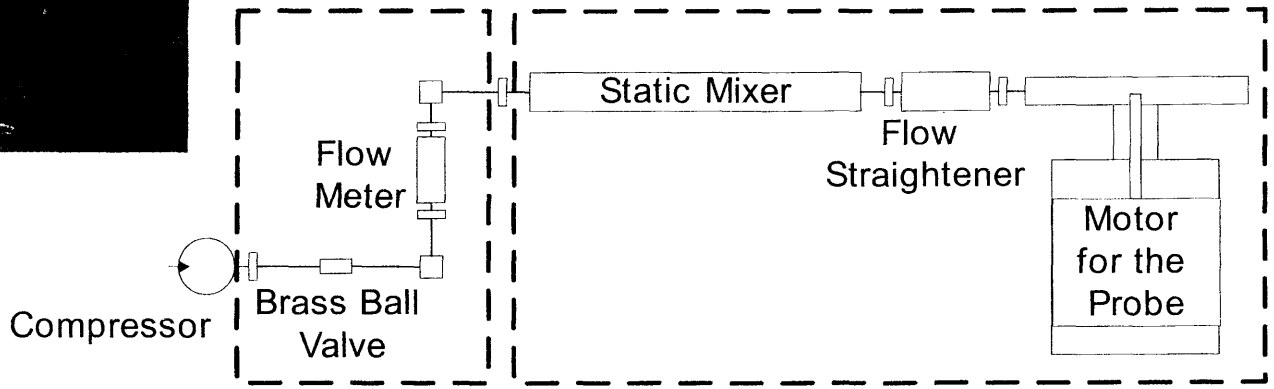

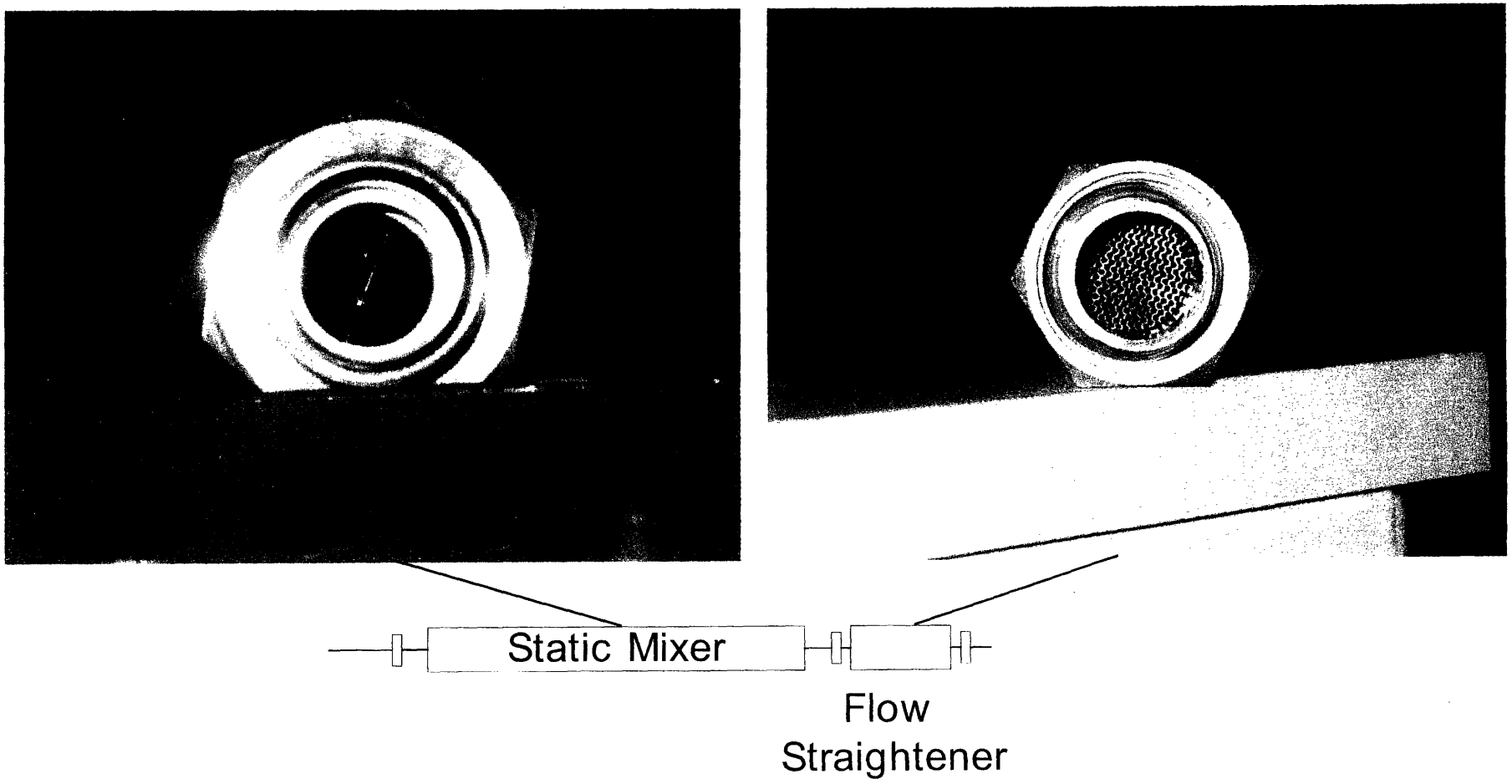
Static Mixer
Flow
Straightener

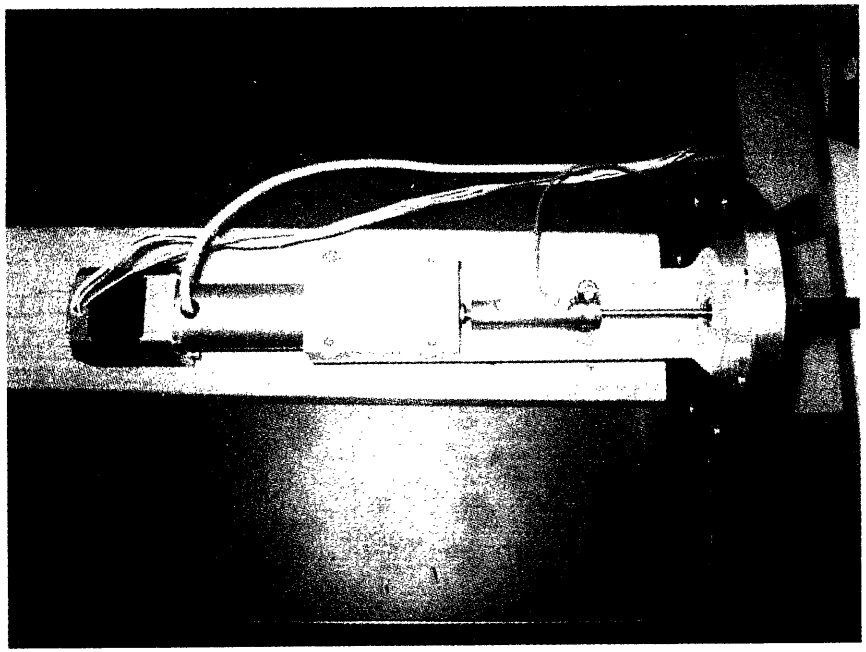

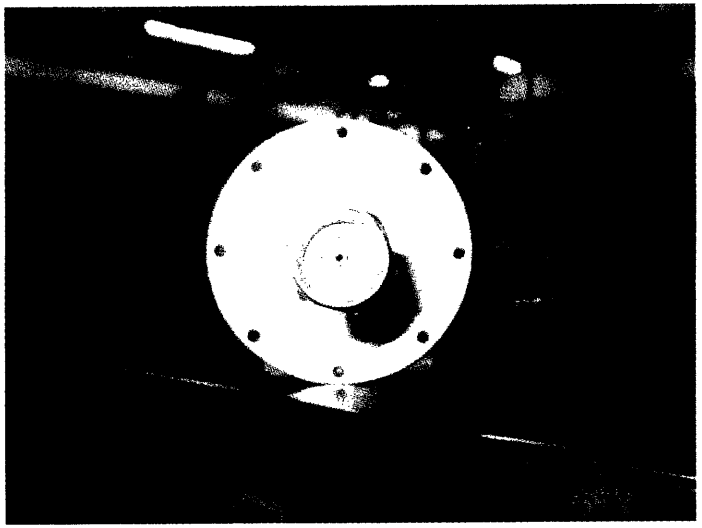

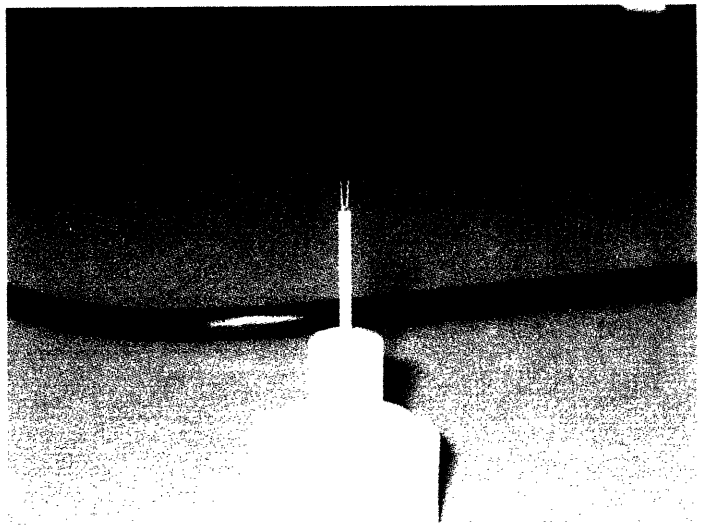

Hot-Wire and Transverse System

APPENDIX B : L-S MODEL UDF

This is the User Defined Function (UDF), which the author wrote to implement the Launder-Sharma model into FLUENT 6.1.22. The basic programming language is C.

```
#include "udf.h"
/* User-definedscalars */
enum
{
        rootK,
        DUDY,
        DVDX,
        DWDX,
        N_REQUIRED_UDS
};

/************************************************************************/
/* UDF for specifying a k source term for Launder-Sharma Model        */
/************************************************************************/

DEFINE_SOURCE(k_source, c, t, dS, eqn)
{
real source;
real x[ND_ND];

C_CENTROID(x,c,t);
C_UDSI(c,t,rootK)=sqrt(C_K(c,t));


source=-
2.0*C_MU_L(c,t)*(pow(C_UDSI_G(c,t,rootK)[0],2.0)+pow(C_UDSI_G(c,t,rootK)[1],2.0)
+pow(C_UDSI_G(c,t,rootK)[2],2.0));
dS[eqn]=-
(C_MU_L(c,t)/C_K(c,t))*(C_UDSI_G(c,t,rootK)[0]+C_UDSI_G(c,t,rootK)[1]+C_UDSI_
G(c,t,rootK)[2]);

return source;
```

```
}

/************************************************************************
*/
/* UDF for specifying a epsilon source term for Launder-Sharma Model        */
/************************************************************************
*/

DEFINE_SOURCE(eps_source, c, t, dS, eqn)
{
real source;
real Re;
real con, DUDYDZ, DVDXDZ, DWDXDY;
real x[ND_ND];

C_CENTROID(x,c,t);
C_UDSI(c,t,DUDY)=C_DUDY(c,t);
C_UDSI(c,t,DVDX)=C_DVDX(c,t);
C_UDSI(c,t,DWDX)=C_DWDX(c,t);
DUDYDZ=C_UDSI_G(c,t,DUDY)[2];
DVDXDZ=C_UDSI_G(c,t,DVDX)[2];
DWDXDY=C_UDSI_G(c,t,DWDX)[1];
con=2.*(DUDYDZ*DUDYDZ+DVDXDZ*DVDXDZ+DWDXDY*DWDXDY);

Re=C_R(c,t)*C_K(c,t)*C_K(c,t)/C_MU_L(c,t)/C_D(c,t);

source=M_keC1*0.3*exp(-
Re*Re)*C_R(c,t)*C_D(c,t)*C_D(c,t)/C_K(c,t)+2.0*C_MU_L(c,t)*C_MU_T(c,t)/C_R(c,t)
*con;
dS[eqn]=M_keC1*0.3*exp(-Re*Re)*C_R(c,t)*C_D(c,t)/C_K(c,t)*(1.+Re*Re)-
2.0*C_MU_L(c,t)*C_MU_T(c,t)/C_R(c,t)/C_D(c,t)*con*(1.+3.5/50.*Re/(1.+Re/50.)/(1.+
Re/50.));

return source;
}

/************************************************************/
/* UDF for specifying a mu_t for Launder-Sharma Model        */
```

```
/************************************************************/

DEFINE_TURBULENT_VISCOSITY(user_mu_t, c, t)
{
real mu_t;
real Re;

Re= C_R(c,t)*C_K(c,t)*C_K(c,t)/C_MU_L(c,t)/C_D(c,t);
mu_t=M_keCmu*C_R(c,t)*C_K(c,t)*C_K(c,t)/C_D(c,t);
mu_t=mu_t*exp(-3.5/(1.+Re/50.));

return mu_t;
}
```